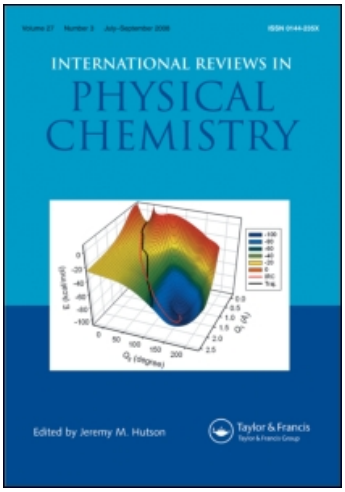

International Reviews in Physical Chemistry
Publication details, including instructions for authors and subscription information:
http://www.informaworld.com/smpp/title~content=t713724383

Vibrational spectra and point defect activities of icy solids and gas phase clusters

J. Paul Devlin[a]
[a] Department of Chemistry, Oklahoma State University, Stillwater, Oklahoma, USA

To cite this Article Devlin, J. Paul(1990) 'Vibrational spectra and point defect activities of icy solids and gas phase clusters', International Reviews in Physical Chemistry, 9: 1, 29 — 65
To link to this Article: DOI: 10.1080/01442359009353237
URL: http://dx.doi.org/10.1080/01442359009353237

INTERNATIONAL REVIEWS IN PHYSICAL CHEMISTRY, 1990, VOL. 9, NO. 1, 29–65

Vibrational spectra and point defect activities of icy solids and gas phase clusters

by J. PAUL DEVLIN
Department of Chemistry, Oklahoma State University, Stillwater, Oklahoma, U.S.A.

This review focuses on the vibrational spectra of icy solids, in particular ice I, and the value of the spectra in monitoring point defect activity within the various hydrogen-bonded networks. After a brief review of the spectra of icy substances containing only H_2O or D_2O, an attempt is made to update both the spectroscopic data and the interpretation by emphasizing recent results for isotopically diluted/decoupled D_2O in H_2O ice I, amorphous ice and the clathrate hydrates. These data are informative of the magnitude of the intramolecular and intermolecular O–H oscillator coupling strengths, the strength of the Fermi interaction between ν_1 and $2\nu_2$, the influence of symmetric hydrogen bonding on the directionality of the water-molecule bond-dipole-moment derivative, and, perhaps most importantly, the spatial extent of the collective vibrations in icy substances. The interpretation of the spectra retains, and expands, the assignment of Whalley (1977) based on the view that intermolecular coupling forces, caused by hydrogen bonding (ν_1) and the polarization field (ν_3), give rise to collective oscillations that dominate the appearance of the infrared and Raman stretching-mode band complexes.

The classical conductivity data for icy substances is generally understood in terms of the combined activity of ionic and orientational point defects. The incorporation of a water isotopomer (e.g. D_2O) in the icy network of a second (H_2O) is possible because such point defect activity, required for isotopic exchange, is lacking at very low temperatures. The simplicity and uniqueness of the spectra of the isotopically decoupled units allows monitoring of the $[D_2O]$, [HOD] and $[(HOD)_2]$. Consequently, after an isotopomer is incorporated within an icy substance, isotopic exchange, stimulated by one of several approaches, may be monitored. A review of the data for the point defect activities for several icy substances suggests that the theory developed by Jaccard (1959) and others from classical conductivity data is basically correct. However, a modification appears to be necessary to account explicitly for an activation energy for the proton hopping which results from intrinsic shallow trapping of the protons. A limited review of the concept, that crystallization rates of icy substances are dependent on the activity of L-defects, identifies a need for additional study.

1. Introduction

The spectroscopic study of ice I, amorphous ice and, to a lesser degree, the clathrate hydrates reached a turning point a decade ago. Infrared, far-infrared and Raman spectra of high quality had been published for each case and the characteristics of the spectral patterns were well known. It was recognized that the spectra of each of these substances in the water-molecules fundamental and torsional mode regions were qualitatively similar with (*a*) extremely broad complex band systems in the O–H (or O–D) stretching mode region, (*b*) broad weak ill-defined absorption/scattering in the bending mode region and (*c*) strong, broad and nearly structureless torsional mode bands. It was further appreciated that proton disorder was a source of band breadth for ice I and the clathrate hydrates while the amorphous-ice bands are inhomogeneously

0144-235X/90 $3·00

broadened. Also, since the O–H (O–D) stretching complex was observed to collapse to a *relatively* narrow and nearly structureless feature for HOD isolated in D_2O (H_2O), it was clear that some combination of intramolecular and intermolecular dynamical coupling of the O–H oscillators was responsible for most of the breadth and structure of the stretching-mode band complex.

Quantitative evidence of the strength of the intermolecular coupling was available from the magnitude of the splitting between the in- and out-of-phase O–H stretching modes of neighbour-coupled $(HOD)_2$ units isolated in H_2O ice I (Haas and Hornig 1960). Missing was direct evidence of the magnitude of the intramolecular coupling of O–H oscillators in an icy environment (i.e. the source of the splitting of the symmetric and antisymmetric stretching modes of the water molecule) and a clear understanding of the distance over which the collective modes, based on intermolecule coupling, extend.

With nearly complete spectroscopic data in hand, the time was appropriate for the development of a more insightful interpretation of the ice spectra. Whalley (1977) responded by combining ideas regarding intermolecular coupling, that had evolved within his group, with projected analogies between the dynamics of ice I and amorphous ice and the proton ordered ices. Although the available data did not allow a confident quantitative division of the dynamical coupling into intra- and intermolecular components, Whalley was able to develop an assignment of the major features of the vibrational spectra of ice and amorphous ice, an assignment which has largely stood the test of time. At about the same time, Rice's group, following a detailed study of the Raman and infrared spectra of ice I and amorphous ice (Sivakumar *et al.* 1977, 1978a), presented the first of a series of theoretical analyses of ice spectra (McGraw *et al.* 1978) which have affirmed that the breadth and distribution of vibrational modes, and of intensity in the Raman and infrared spectra, are dominated by the influence of intermolecular coupling, with an apparently more modest effect from Fermi resonance.

In a somewhat similar manner, classical studies of point defect activity in icy substances also reached a turning point in the same decade. As thoroughly reviewed by Hobbs (1974), studies of both direct and alternating current conductivities, as well as dielectric relaxation times, for ice I_h at various levels of purity had been reported and the theory developed by Jaccard (1959), and others, parameterized. This theory, and most of the thinking, was based on the concept of a two-step proton conduction mechanism with net proton transport dependent on sequential proton hopping and orientational defect migration, a mechanism similar to the Grotthuss mechanism for proton transport in liquid water. This model, in combination with the conductivity data, indicated that for pure ice I_h the hopping rate, which is dependent on $[H^+]$, is slow and, therefore, rate-determining at high ice temperatures whereas the more strongly activated orientational-defect motion is rate-determining at temperatures much lower than 200 K. Since it can be argued that the slow step determines the observed d.c. conductivity whereas the fast step dominates the a.c. conductance, the rates and activation energies for the two steps could be deduced separately.

The essence of Jaccard's theory is apparently gaining affirmation with time, but the situation a decade ago was not that satisfactory. There was no molecular-level experimental evidence of the existence of two essentially independent point defect systems, namely the ionic and orientational (or Bjerrum) defects. Also, there were significant inconsistencies within the available conductivity and dielectric constant data, and the extension of the classical measurements to lower temperatures, as a means

of affirming trends and testing predictions, was blunted by inadequate d.c. signals and an apparent dominance of the a.c. conductivity by extrinsic charge carriers from ice impurities. Theoretical efforts to simulate the behaviour of point-defect activities were only beginning to provide useful qualitative insights (Plummer 1978).

From the above we see that a decade ago molecular-level models existed that provided reasonable and, apparently, basically correct interpretations of both the spectroscopic and the conductivity data for icy substances but, because critical observations were missing, the images were clouded and uncertain. The complexity of the ice spectra is such that a confident analysis is impossible without direct experimental evidence of the relative importance of intermolecular and intramolecular coupling, the influence of Fermi resonance between ν_1 and $2\nu_2$ and deeper insight into the delocalized character of the vibrational excitons. Jaccard's theory of point defect activities was elegant, but contestable in the absence of direct evidence of the separate existence of ionic and orientational defects. The purpose of this review is to examine advances in our understanding of both the vibrational spectra and the point-defect activities of icy substances during the present decade. The emphasis will be on spectroscopic data which have become available through the development of techniques to 'isolate' D_2O in protiated ices, and *vice versa* (Ritzhaupt *et al.* 1978, 1980). Isolated D_2O molecules (i.e. D_2O incorporated intact in a largely H_2O lattice) serve as an excellent spectroscopic probe of both relative coupling strengths and of the point defect activities, a situation that binds together the study of the spectra and the point-defect activities of icy substances. Theoretical developments related to these subjects have also been substantial, contributing in particular to our understanding of the ice spectra. However, fairly recent reviews have stressed these developments (Sceats and Rice 1982, Rice *et al.* 1983) so they will be cited here primarily in the context of the experimental data.

The emphasis in this review will, at least initially, be on the properties of crystalline proton-disordered ice I. This label could apply to either cubic or hexagonal ice (i.e. ice I_c or ice I_h), so some ambiguity is implied, perhaps appropriately since the transition from cubic to hexagonal ice has been characterized as the healing of hexagonal stacking faults (Carmona *et al.* 1989). Generally, crystalline ice samples prepared below ~ 180 K at low pressures can be presumed to be cubic in form, while samples which have existed for a significant period at temperatures above 200 K assume a hexagonal structure. However, much of the information to be examined was obtained for samples for which individual structural characterization, as either hexagonal or cubic, was not practical. Spectroscopically this is not viewed as a serious weakness since no distinction between the internal-mode spectra of the two ice I forms has ever been established. It is perhaps more important to keep in mind that the studies of defect mobilities, through the monitoring of the spectra of isolated isotopomers, were for samples prepared below 130 K and, therefore, almost certainly cubic in form. The properties of amorphous ice and the clathrate hydrates are best understood in the context of what is known about ice I, so are reviewed accordingly. Unless otherwise indicated the term 'amorphous ice' refers to the low-density form as typified by samples prepared by vacuum deposition at temperatures near 100 K or by the 120 K annealing of high-density amorphous ice, originally prepared by pressurizing ice I (Handa and Klug 1988).

2. Vibrational spectra of icy solids and clusters

In this section, an overview is provided of the spectroscopic data of icy substances, along with a current interpretation of the data and a brief look at the implications of

that interpretation for the structure of water. In part 2.1, a brief review of the state of knowledge of the spectra of ice and the clathrate hydrates which existed a decade ago is provided, as a background to a discussion of recent developments which have enhanced that understanding (part 2.2). From an experimental viewpoint many of the advances have stemmed from the development of techniques for the growth of a variety of icy substances at temperatures below 120 K. At such temperatures, point defects within icy substances are either extremely rare or inactive, or both, so no mechanism exists for isotopic exchange (see section 3). This facilitates the incorporation of a few molecules of one isotopomer (e.g. D_2O) within the 'lattice' of a second (e.g. H_2O), so that the fundamental modes of the dilute isotopomer are isotopically decoupled from the modes of neighbouring vibrators. Attention will be focused on the interpretations made possible by the gross simplification of the spectra of icy substances which results from such decoupling.

In section 2.3, attention is drawn to the spectra of large neutral gas-phase *clusters* of icy substances which have been reported only recently (Devlin 1989, Fleyfel and Devlin 1990). The dependence of the structural phases of such clusters on experimental parameters, as deduced from comparisons of the cluster spectra with the spectral patterns described in section 2.1, will be reviewed. Variations in the cluster spectra, from the known spectra of the corresponding bulk phases of ice, will also be emphasized. For several years the spectra of icy substances and, in particular, amorphous ice have been viewed as a likely source of insight to the vibrational spectra and structure of liquid water and aqueous solutions. The understanding of the amorphous-ice spectrum has reached a level where such a transfer of information has become feasible. One example of that transfer, as achieved by Sceats and co-workers (Green *et al.* 1986a, b, 1987), will receive particular attention in section 2.4.

2.1. *Ice I, amorphous ice and clathrate hydrates: pre-1980*

There are numerous sources of excellent infrared and Raman spectra of crystalline ice I. Rice and Sceats and their co-workers (1982, 1983) have presented superlative reviews of the spectra which were published before about 1980, while also providing a detailed comparison with the predictions of the most complete available theory of the spectra of icy substances. For the most part, it is not practical to seek to improve on their examination of those data. Rather, an attempt is made here to focus on a limited number of representative spectra which demonstrate distinct characteristics of icy substances, so as to develop a framework for understanding the more recent data. For example, the juxtaposition of the polycrystalline ~90 K infrared and Raman spectra in the O–H stretching mode region for H_2O ice I in figure 1 (Wong and Whalley 1975) shows the complex nature of the ice spectra in the stretching mode region as intensity is divided between several subbands having positions ranging from below 3000 cm^{-1} to above 3400 cm^{-1}. This figure also reveals the markedly different distribution of intensities observed for absorption and scattering.

The most prominent of the ice subbands is the strong Raman feature near 3083 cm^{-1}, a position lower in frequency than over 90% of the infrared band intensity. This intense Raman feature, which seems to be a key to understanding the spectra/structure of icy substances and water, is known to be highly polarized, as is clear from the single crystal 167 K spectrum of ice in figure 2 (Scherer and Snyder 1977), which also reveals the sizeable anisotropy in other components of the Raman band (i.e. particularly at 3209 and 3323 cm^{-1}). A comparison of the single crystal cc polarizability component (i.e. component of light, with electric vector along the crystal

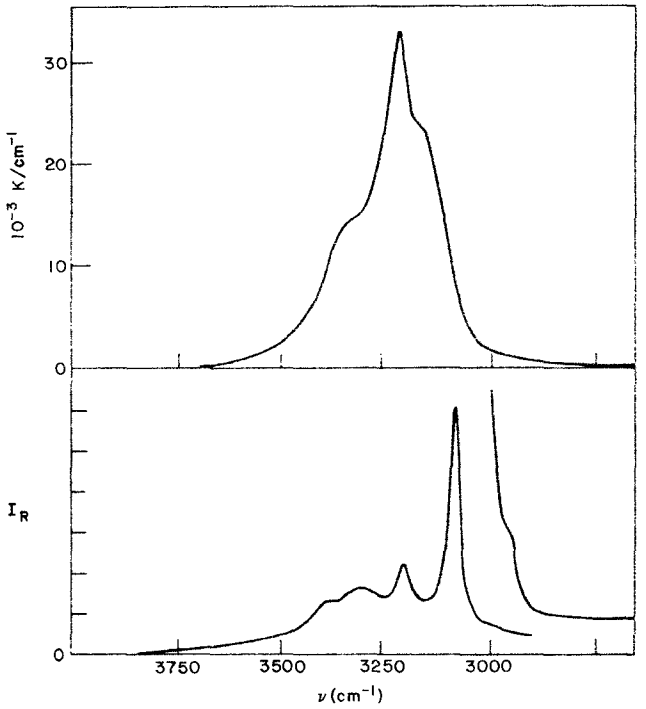

Figure 1. A comparison of the infrared (upper frame) and Raman (lower frame) spectra of ice I_h in the same frequency scale (Wong and Whalley 1975).

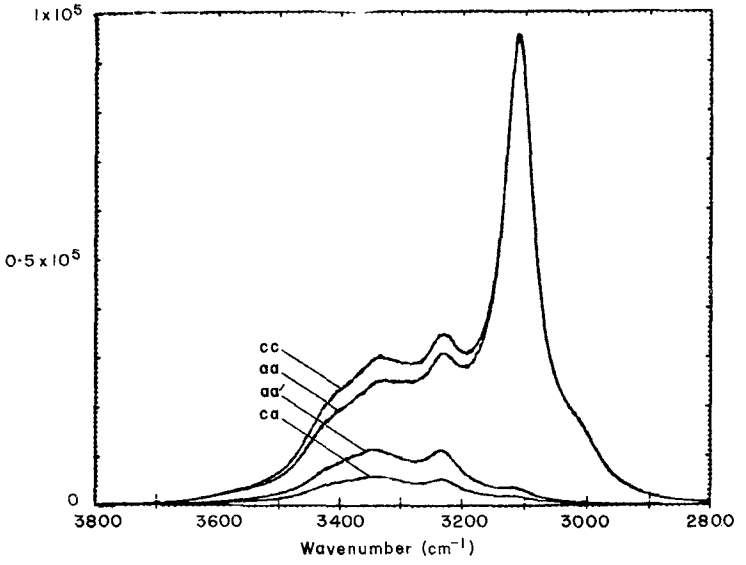

Figure 2. Raman spectra of single crystal H_2O ice I_h at $-106°C$ (Scherer and Snyder 1977).

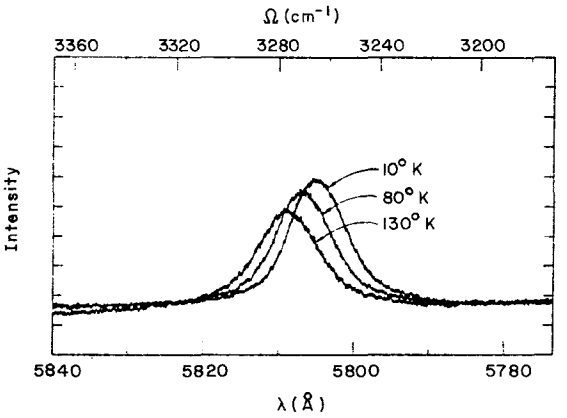

Figure 3. The Raman spectrum of polycrystalline HOD in D_2O ice I (1·5% HOD) as a function of temperature (Sivakumar *et al.* 1977).

c axis, scattered from light polarized in the *c* axis direction) with the polycrystalline Raman spectrum of figure 1, which was obtained at a temperature lower by nearly 80 K, also reveals that the general form of the spectrum changes significantly with temperature. Upon close inspection, the thoroughly documented shift of each band component to a higher frequency with increasing temperature (Wong and Whalley 1975, Sivakumar *et al.* 1978a) is apparent. The temperature effect, which is particularly large for the 3083 cm^{-1} feature and the other 'sharp' component at 3209 cm^{-1}, is generally attributed to a lengthening of the ice hydrogen bond which, because of bond anharmonicity, accompanies increased lattice vibrational motion.

A similar but smaller temperature effect is observed for the ν_{OH} mode of isotopically decoupled HOD (figure 3). Because of the exceptional temperature dependence of the positions of the band components of both the infrared and Raman band complexes in the stretching mode region of ice, amorphous ice and the clathrate hydrates, the identification of band peak frequencies, without stating the temperature, is of little value. For that reason throughout this review all reported frequencies are for spectra measured at approximately 90 K unless a different temperature is specified. A similar dependence of Raman band positions on pressure has also been documented, as the major features shifts to noticeably lower frequencies for pressures in the kilobar range (Sivakumar *et al.* 1978). Of course a great preponderance of the published spectra are for pressures between 0 and 1 bar.

The ν_{OH} bands of figure 3 also make clear the remarkable reduction in the spread and complexity of the Raman (and IR) band complex which accompanies isotopic decoupling. This effect has been known for decades, and is recognized as a combined result of mass decoupling of the O–H oscillators within the molecule and the mass decoupling of oscillators that are coupled through the hydrogen bonds of the ice lattice. Furthermore, shoulders which emerge on either side of the corresponding ν_{OD} band of HOD isolated in H_2O ice I, when the HOD content exceeds 10% (Haas and Hornig 1960), reflect the coupling strength of near-neighbour HOD molecules. The band positions, at 2442 and 2396 cm^{-1}, indicate a coupling force constant of $\sim -0{\cdot}123 \times 10^5$ dyne cm^{-1}. What is not apparent from these spectra is (*a*) the strength of the *intramolecular* coupling and (*b*) the influence of Fermi resonance and longer-range coupling on the spectra of ice with the oscillators fully coupled (i.e. containing a

single isotopomer). It is understood that for many molecular systems the total exciton splitting of internal modes from intermolecular coupling exceeds that of near-neighbour coupling by a large factor (Zhizhin and Goncharov 1984), but the significance of this longer range coupling to the spectra of the proton-disordered ices was not apparent from experimental data until very recently (see section 2.2.2).

Studies of the spectra of deuterated ices have been nearly as extensive as for protiated ices. The stretching-mode band complex in the 2400 cm^{-1} region is similar to that of the H_2O ices in most obvious respects with the situation for hexagonal ice demonstrated in figure 4. The form of the Raman spectra of deuterated ice, as well as subtle differences compared to protiated ice, will be made somewhat clearer in section 2.2.2 on the stepwise isotopic dilution of H_2O ice with D_2O.

One of the real surprises in the study of ice spectra has been the discovery that the patterns of the vibrational spectra of amorphous ice, and in particular, the Raman spectra of the stretching modes, are remarkably similar to those of crystalline ice. This similarity can be noted from a comparison of the 110 K Raman spectra of amorphous and polycrystalline ice in figure 5 (*a*); and the amorphous-ice scattering patterns for different polarizations in figure 5 (*b*) (Li and Devlin 1973) compared with those of figure 2. The isotropic character of the scattering near 3100 cm^{-1} is clearly retained by amorphous ice. The most notable differences, compared to the crystalline-ice spectra, are caused by the sensitivity of the stretching mode frequencies to the hydrogen-bond strength as reflected in the O–O distances. A greater range of O–O distances contributes to an increased width of the band components of amorphous ice while an increased average O–O distance is reflected in a shift of the positions of the band

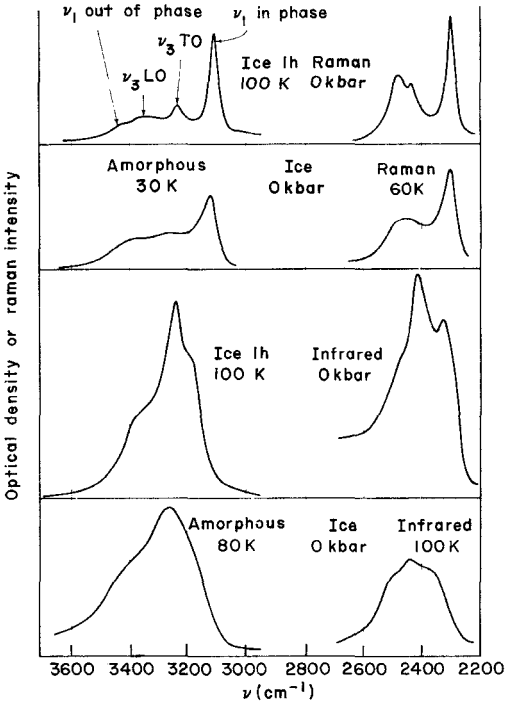

Figure 4. Infrared and Raman spectra of ice I_h and amorphous ice under conditions as indicated (Whalley 1977).

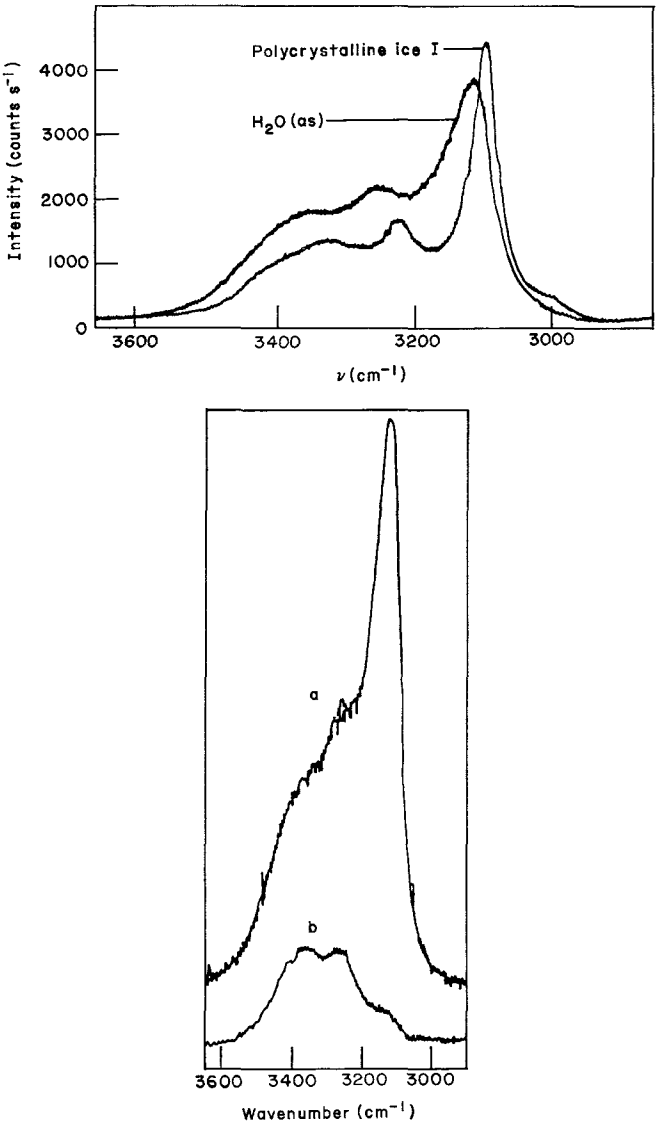

Figure 5. A comparison of Raman spectra of amorphous and polycrystalline ice at 110 K (Sivakumar *et al.* 1978c) and (lower frame) parallel and perpendicularly polarized Raman scattering of amorphous ice at 90 K (Li and Devlin 1973).

components to higher frequencies. The greater bandwidth is readily appreciated by a comparison of the f.w.h.m. of the O–D stretching mode of decoupled HOD in amorphous ice ($\sim 70\,cm^{-1}$) with that of crystalline ice ($< 20\,cm^{-1}$).

Early studies of the spectra of the icy host lattice of the clathrate hydrates (structure I and structure II) revealed the similarity of the spectra to that of ice I, in both the internal and external mode regions (Bertie and Othen 1972, 1973, Johari and Chew 1983). The clathrate hydrate spectra may be most simply characterised by noting that the bands of the fundamental water-molecule modes have an appearance between that

of ice and amorphous ice in many respects. The f.w.h.m. tends to be slightly less than for amorphous ice, while the peak positions tend to be shifted slightly from the ice values towards the amorphous ice positions. A f.w.h.m. greater than ice I is understandable since, like ice, the clathrate hydrates are proton-disordered but do not have a 'single' equilibrium O–O near-neighbour distance (Davidson 1973). Since the average O–O distance is slightly greater than for ice I, the shift to higher frequencies of the stretching mode band components is also anticipated. However, in section 2.2.4 an example (TMO: structure I) will be noted where a subset of the O–O distances gives rise to stretching-mode band positions lower in frequency than those of ice I.

2.2. *Decoupled D_2O, H_2O and $(HOD)_2$ spectra*

The usefulness of a few per cent of HOD as a probe of the structure of icy substances has been appreciated for decades. Though the decoupling of an HOD vibrational mode from the modes of the dominant isotopomer (H_2O or D_2O) is never complete (Rice *et al.* 1983), and effects from coupling to lattice modes are observable (Falk 1987), the residual dynamical coupling can be regarded as insignificant in most contexts. A similar decoupling of oscillators was anticipated for D_2O isolated in H_2O ice, or *vice versa*, as well as the O–H (O–D) stretching modes of units such as $(HOD)_2$ or $(D_2O)_2$ in deuterated (protiated) ice, but it was not recognized that such information is accessible by experimentation. However, during the past decade simple methods have been developed for the preparation of crystalline, amorphous and clathrate hydrate icy samples containing a few per cent of a second water isotopomer at temperatures sufficiently low that isotopic exchange is inhibited (Ritzhaupt and Devlin 1977, Ritzhaupt *et al.* 1978, 1980, Richardson *et al.* 1985a). Spectroscopic data from such samples are informative of (*a*) the magnitude of the *intramolecular* coupling of water molecules in an icy substance, (*b*) the spatial extent of the collective vibrations in ice and the influence of long-range coupling on the observed spectra, (*c*) the role of Fermi resonance in shaping the observed stretching-mode band complexes and (*d*) the directionality of the water-molecule bond dipole-moment derivatives.

Most of the data to be examined in this section has been made available by this simple expedient of growing the samples at temperatures sufficiently low that point-defect activities are suppressed, so that isotopic-exchange rates approach zero. However, the observation of the decoupled modes of $(HOD)_2$, without interference, requires a more sophisticated control of the point-defect activities. As will be made clear in section 3.3, the stimulation of proton activity, in the absence of any orientational (Bjerrum) defect motion, converts isolated D_2O (or H_2O) to isolated neighbour-coupled $(HOD)_2$.

2.2.1. *Isotopomers decoupled in crystalline ice I*

By the co-deposition of a dilute stream of D_2O molecules with a dense vapour stream of H_2O at 125 K, D_2O molecules can be isolated intact in H_2O ice, with only minor HOD contamination. The crystalline character of the deposit can be guaranteed by using an ultrathin film of H_2O ice I, pre-deposited at 160 K, as a substrate for epitaxial growth (Collier *et al.* 1984). Since the spectrum of decoupled HOD is well known (figures 3 and 6(*c*)), its influence on the deposit spectrum can be removed using Fourier-transform infrared (FTIR) difference techniques. The resulting D_2O spectrum in the stretching mode region is shown as curve (*a*) of figure 6, and the peak frequencies and bandwidths are included in the table which also contains data for other units isolated/decoupled in ice I. Conversion of the decoupled D_2O molecules to $(HOD)_2$, by

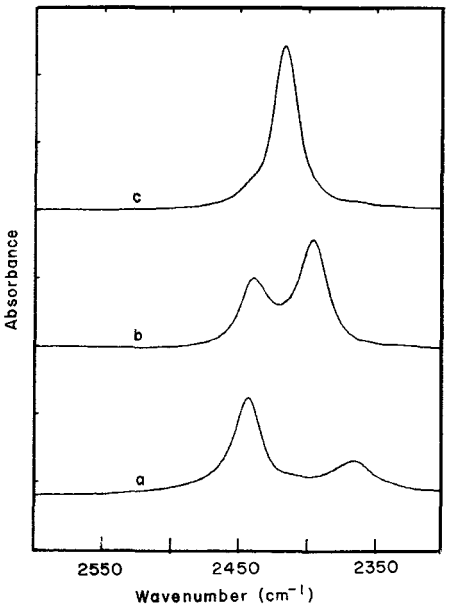

Figure 6. Infrared spectra for isotopomers of H_2O decoupled in H_2O ice at 90 K: (*a*) D_2O; (*b*) $(HOD)_2$; (*c*) HOD (Devlin *et al.* 1986).

The observed vibrational frequencies (cm^{-1}) of decoupled isotopomers in cubic ice at 90 K. The unperturbed (ν_s and z) and calculated perturbed $\nu^{\pm}$ vibrational frequencies of the Fermi diads are also included. F.w.h.m. bandwidths are indicated in parenthesis along with the major component of the ice sample, where ambiguous.

	H_2O	D_2O	HOD	$(HOD)_2$
ν_3 (obs.)	3270 (~40)	2443 (20)		
ν_{OH}^{+}/ν_{OH} (obs.)			3270 (30)	3299 (50)
				3238 (50)
ν_{OD} (obs.)			2417 (20)	2442 (22)
				2396 (23)
ν_1 (obs.)	3225 (~70)	2366 (33)		
ν_1^{-} (calc.)	3227	2365		
ν_s	3244	2391	3257	
ν_2 (obs.)	1735 (~50)	1225 (~45)	1510 (in D_2O; 20)	
			1490 (in H_2O)	
$2\nu_2$ (obs.)	3435 (~100)		~2970† (in D_2O)	
			~2940 (in H_2O)	
$2\nu_2^{\pm}$ (calc.)	3455	2458	2983	
z	3436	2432	2996	

† Estimated by adding 30 cm^{-1} to the amorphous ice value (see text).

artificial stimulation of the proton hopping activity (Wooldridge *et al.* 1987, Wooldridge and Devlin 1988), results in a clear view (figure 6(*b*)) of the doublet of the in- and out-of-phase modes of neighbour-coupled HOD molecules, which was originally observed as indistinct shoulders by Haas and Hornig (1960).

The splitting of peak positions of the D_2O doublet (figure 6(*a*)) might be interpreted as an indication of the coupling strength of the intramolecular O–D oscillators. However, as discussed by Scherer (1978) and analyzed by Sceats *et al.* (1979) the influence of Fermi resonance, between the bending mode overtone and the symmetric stretching mode, must be established before the frequency of the unperturbed ν_1 mode is apparent. The corrected ν_1 frequency is included as ν_s in the table from which the ν_3–ν_s splitting from *intramolecular* coupling can be determined as 52 cm^{-1}, indicative of a bond–bond interaction force constant of $\sim 0{\cdot}06$ mdyne $Å^{-1}$. The magnitude of the *intermolecular* coupling constant can also be deduced from the 46 cm^{-1} splitting of the $(HOD)_2$ doublet components in figure 6(*b*). Since this splitting is less than the 49 cm^{-1} value estimated by Haas and Hornig, the coupling constant is slightly less negative than their value of $-0{\cdot}123 \times 10^5$ dyne cm^{-1}.

The value of $\sim 1{\cdot}75$ for the ratio of the D_2O integrated band intensities of the antisymmetric and symmetric modes (figure 6(*a*)), which is reduced by an order of magnitude from the gas phase values, has been used by Whalley and Klug (1986) to establish the direction of the dipole-moment derivative for the O–D (O–H) bond in ice. They find that the derivative is nearly along the bond, in marked contrast to an off-bond angle of 25° for water vapour. Similarly, the ratio of intensities of the bands of the in-phase and out-of-phase O–D modes of $(HOD)_2$, which has been estimated as 1·66 from figure 6(*b*), is indicative of an angle of $\sim 3°$ between the bond and the derivative (Whalley and Klug 1987), confirming the dramatic effect of hydrogen bonding on the electron distribution as reflected in this molecular parameter.

The spectra for H_2O and $(HOD)_2$ decoupled in D_2O ice are presented in figure 7. For reasons that are well understood, these spectra are not as attractive or revealing as those of figure 6. There is an increased overlapping of the spectral features, because of the inherently greater bandwidth of the O–H vibration and because the splitting of the unperturbed symmetric and antisymmetric stretching mode frequencies of H_2O is much less than for D_2O (Sceats *et al.* 1979). A specific effect of this small splitting, combined with Fermi resonance between ν_{OH} and $2\nu_2$ of decoupled HOD, is a coincidence of ν_3 of H_2O with the observed ν_{OH} of HOD. The values for the decoupled frequencies are summarised in the table which also includes the results from a unified fitting of the various unperturbed isotopomer-stretching mode frequencies to the observed data using a Fermi-interaction parameter of 60 cm^{-1} for H_2O and the indicated bending-mode frequencies (Devlin *et al.* 1986).

The isolated isotopomer bending mode frequencies shown in the table have been (and may remain) the source of some controversy. There seems to be little debate of the value of D_2O (~ 1225 cm^{-1}) though it is recognized that the band complex in that region of the spectrum also contains a torsional overtone component. The value of HOD (1510/1490 cm^{-1}) seems to be accurate, since a new distinct feature appears, without interference, in both infrared and Raman spectra of samples containing significant amounts of HOD. The uncertainty has resided in the value deduced for isolated H_2O from ice samples containing 5–10% of H_2O in D_2O ice. In two different studies in two different laboratories, a weak feature at 1735 cm^{-1}, which disappears upon isotopic scrambling, has been assigned to the bending mode (Ritzhaupt *et al.* 1980, Bertie and Devlin 1984). However, it has been argued that a frequency greater

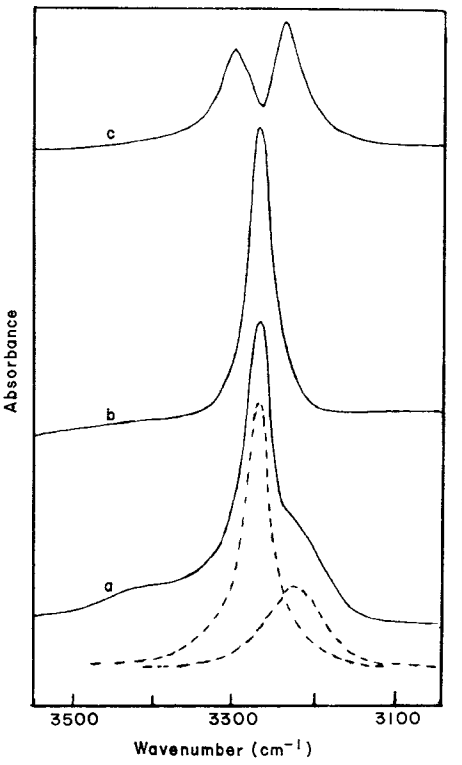

Figure 7. Infrared spectra for isotopomers of D_2O decoupled in D_2O ice at 90 K: (*a*) H_2O; (*b*) HOD; (*c*) $(HOD)_2$ (Devlin *et al.* 1986).

than 1700 cm^{-1} is unacceptable, and that an attempt to use such a value, in an analysis of the stretching mode region, must lead to unacceptably large values of the Fermi-interaction parameter (Efimov 1982).

The acceptability of the 1735 cm^{-1} value for ν_2 is enhanced by the fact that Falk's empirical equation, relating ν_2 to ν_{OH} for decoupled isotopomers, predicts a value of 1703 cm^{-1} for ice I (Falk 1984). It has also been shown that, after accounting for the Fermi-resonance effect on HOD ν_{OH} band position, the need for an oversized Fermi-interaction parameter, which is otherwise required by the ν_2 value of 1735 cm^{-1}, is eliminated (Devlin *et al.* 1986). Finally, the most recent thorough theoretical analysis of the spectrum of ice has invoked the value of 1735 cm^{-1} as the ν_2 value for decoupled H_2O (Bergren and Rice 1982), and a very recent paper on the decoupled ν_2 mode of amorphous ice shows an observed value of 1711 cm^{-1} which is qualitatively consistent with the Falk equation and the ice value of 1735 cm^{-1} (Devlin 1989a).

The observed decoupled fundamental frequencies, the values corrected for Fermi interaction and the frequencies for neighbour-coupled $(HOD)_2$ modes listed in the table seem to be the best experimental basis for attempts to analyze the coupled-mode spectra of pure H_2O or pure D_2O ice I. However, these data do not give any new insight to the spatial extent of the collective modes in ice. What is missing is a comparison of the frequencies of neighbour-coupled pairs of D_2O (or H_2O) molecules with the frequencies of progressively larger aggregates of one isotopomer imbedded in the matrix of the other. This comparison is given in the next section.

2.2.2. *Isotopomers diluted in crystalline ice I*

The same experimental approach that allows the incorporation of a few per cent of one isotopomer within the icy lattice of a second isotopomer can also be used to prepare icy samples containing any desired percentage content of H_2O and D_2O. This means that the intermolecular coupling of water molecules in ice can be observed for D_2O (or H_2O) aggregates ranging in size from $(D_2O)_2$ units to the complete icy sample. Spectra reflecting the varying isotopomer aggregate sizes have been obtained (Devlin 1989) and the parallel-polarized scattering for D_2O aggregates presented in figure 8 is particularly informative. (Of course, for each dilution level, there is a complicated distribution of aggregate sizes within a sample).

Figure 8 is better appreciated if it is recalled that the dominant polarized Raman band component at 2287 cm^{-1} in curve (*a*) has long been assigned and accepted as the delocalized in-phase-coupled ν_1 mode (Wong and Whalley 1975). At the other extreme, curve (*e*) of figure 8, which is basically the Raman spectrum of decoupled D_2O, shows the Fermi-resonance-perturbed symmetric-stretching-mode band at 2366 cm^{-1}. An increase of the D_2O content to 20% (curve (*d*)) is accompanied by the growth of a new feature at 2340 cm^{-1} which is assigned to the in-phase-coupled symmetric stretching mode of $(D_2O)_2$. This band position reflects a shift of only 26 cm^{-1} from the decoupled

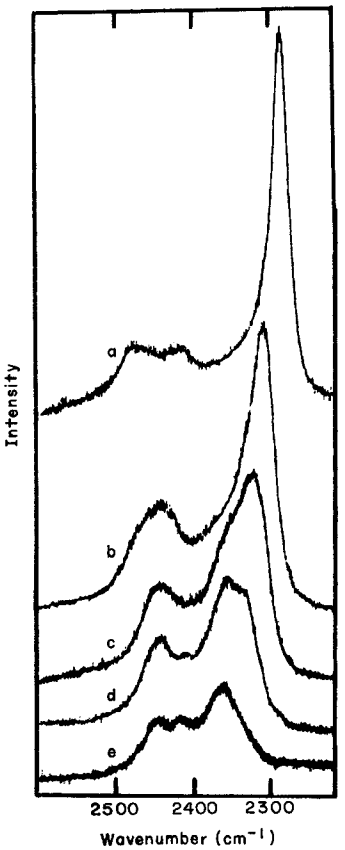

Figure 8. Parallel polarized Raman scattering in the O–D stretching mode region of ice I for various concentrations of intact D_2O. Mole percentage D_2O concentrations are (*a*) 100%; (*b*) 50%; (*c*) 34%; (*d*) 20%; (*e*) 10% (Devlin 1989a).

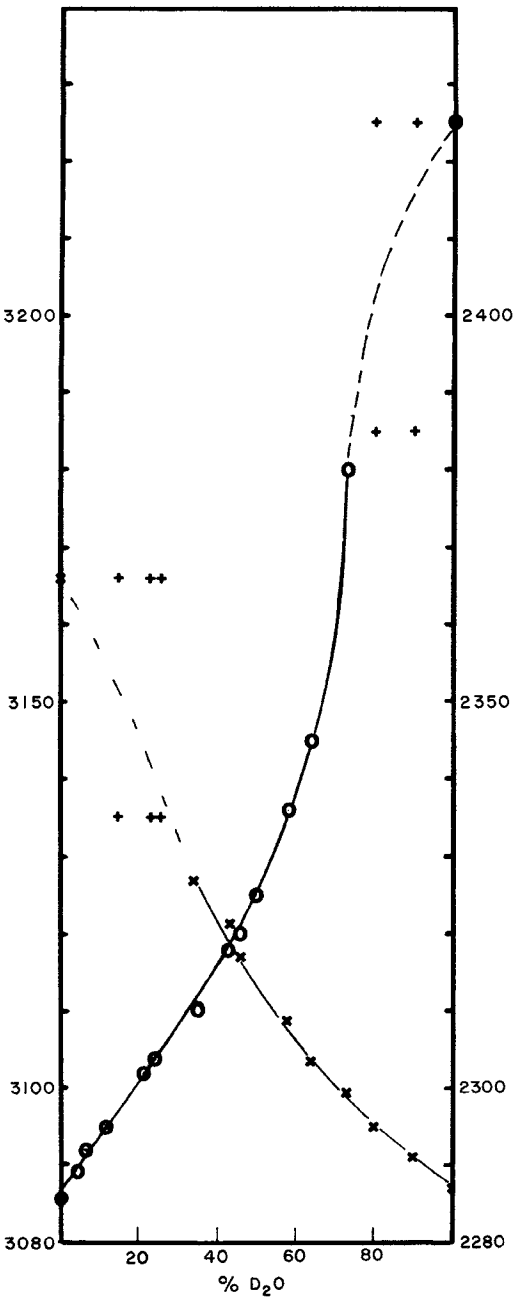

Figure 9. Plots of the peak frequency (cm^{-1}; vertical axis) of the in-phase coupled ν_1 band of H_2O (–O–O–) and D_2O (– × – × –) as a function of the percentage intact D_2O in ice I. The crosses denote component band frequencies for the concentration ranges for which ν_1 appears as a doublet (Devlin 1989a).

value but a further increase of the D_2O content is accompanied by the shift of this Raman band towards the ultimate value of 2287 cm^{-1} for 100% D_2O. Thus, of the total coupling shift of nearly 80 cm^{-1}, ~70% is a result of coupling beyond near-neighbour pairs. This behaviour of the vibrational exciton with isotopomer concentration is similar to that typical of *ordered* molecular crystals and suggests that proton disorder has only a minor influence on the range of the collective motion in ice I.

An impression, that the effect on the magnitude of the coupling shift begins with the first trace of diluent and is nearly linear up to 50% dilution, can be gained from the plot of the observed D_2O (and H_2O) ν_1 peak position against percentage dilution in figure 9. These data seem to indicate that the delocalized resonant coupling of ν_1 is significantly reduced even in large clusters and, therefore, must extend for macroscopic lengths. This amounts to an affirmation of the extreme delocalized character of this mode suggested in the last paragraph.

The effect of dilution on the perpendicularly polarized Raman scattering of H_2O ice is also very interesting. The two dominant features at 3209 and 3323 cm^{-1} in curve (*a*) of figure 10 have enjoyed quite varied assignments over the years. More recently, Whalley (1977) assigned the 3209 cm^{-1} band to the delocalized transverse optical (TO) mode of ν_3 which is also generally presumed to be the source of the nearby, intense infrared band (3220 cm^{-1}). Then, from an analogy with his expectations for ordered cubic ice, he attributed the 3323 cm^{-1} feature to the associated longitudinal optical (LO) ν_3 mode, which was estimated to be at 3299 cm^{-1} from the Lyddane–Sachs–Teller relationship for TO and LO frequencies (Whalley and Klug 1979). An analogous assignment was also suggested for what appears to be the corresponding bands of D_2O ice I with the distinct features at 2427 and 2482 cm^{-1} identified as the ν_3 TO and LO modes respectively. Later, Bergren and Rice (1982), while acknowledging that in principle the ν_3 LO mode may appear in the Raman spectrum of ice, found no evidence of significant longitudinal-mode contribution to the major features of the ice internal-mode spectra. Since a distinct feature did appear near 2420 cm^{-1} in a model calculation that included Fermi-interaction effects between ν_1 and $2\nu_2$, they attributed the experimental maximum in that region to Fermi resonance.

The dilution results of figure 10 are pertinent to this controversy. It seems apparent from these data, and similar data for D_2O, that the components of the doublet in question (3209 and 3323 cm^{-1}) gradually approach a common central position as a result of isotopic dilution, and ultimately converge on the position of the decoupled ν_3 mode at 3270 cm^{-1} (2443 cm^{-1} for D_2O). From an experimental perspective, these two distinct features of the coupled crystalline-ice spectra have their origin in the ν_3 mode of the water molecule with TO/LO splitting the most probable source, considering the great oscillator strength of the ν_3 mode. The observation of transverse and longitudinal bands in the Raman spectra of disordered substances is not unusual and is anticipated for systems wherein the spread of internal-mode frequencies is small compared to the T/L splitting, which is determined by the oscillator strength through the Lindane–Sachs–Teller relationship (Hwang 1974, Devlin and Frech 1975).

2.2.3. *Summary of the interpretation of the ice I data*

The major point that has been emphasized throughout this discussion of the ice spectra is that the breadth and form of the infrared and Raman spectra are caused by and reflect a coupling of oscillators that can be divided into intramolecular and intermolecular in nature. The intramolecular coupling is well determined by the observed splitting of the stretching mode bands of the decoupled isotopomers as

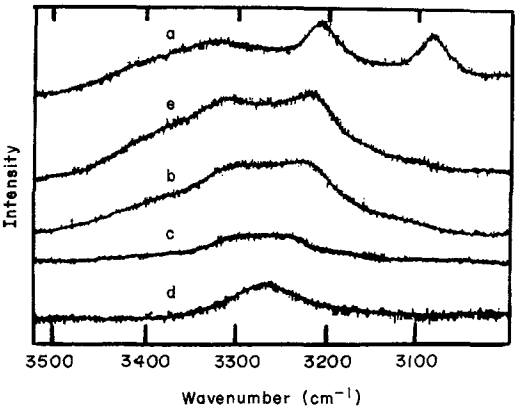

Figure 10. Perpendicularly polarized Raman scattering in the O–H stretching region of ice I for various levels of dilution with intact D_2O. Dilution levels are (*a*) 0%; (*b*) 34%; (*c*) 60%; (*d*) 80%; (*e*) 20%. The band at 3 085 cm^{-1} in curve (*a*) reflects leakage of isotropic scattering intensity (Devlin 1989a).

analyzed by Sceats and Rice. The magnitude of the next-neighbour coupling of oscillators is also apparent from the spectra for the units $(D_2O)_2$ and $(HOD)_2$, and the effects of Fermi resonance on the spectra of the *decoupled* isotopomers is well established. Less obvious are the contributions of Fermi resonance and longer range intermolecular coupling to the fully coupled spectra of ice samples containing a single isotopomer. This is a problem that has been addressed in the theoretical studies of Rice *et al.* but the theoretical results may not fully explain all of the available spectroscopic data.

An apparent divergence of theory and experiment is epitomized by the behaviour of the doublets in the anisotropic scattering spectra at 3209 and 3323 cm^{-1}, and 2427 and 2482 cm^{-1}, for ice I samples of 100% H_2O and 100% D_2O respectively. Attribution of these components to delocalized modes based on the ν_3 vibration is required by the spectroscopic data. The smooth collapse of the doublet onto the position of the decoupled ν_3 mode (figure 8, and similarly for D_2O) rules out a suggested assignement of the maximum in the Raman scattering at 2427 cm^{-1} to a consequence of Fermi resonance (as well as an assignment of either component to a combination mode involving a translational vibration (Scherer and Snyder 1977)). Also, as Wong and Whalley noted, the greater temperature sensitivity of the position of the 3209 cm^{-1} band compared to that of the 3323 cm^{-1} feature is understandable from this ν_3 assignment. The normal shift to higher frequency with increasing temperature would be accelerated for the former and inhibited for the latter by a reduction in the intermolecular coupling (or TO/LO splitting) which must accompany the thermal expansion of ice. It is for a similar reason that the thermal shift of the in-phase ν_1 isotropic Raman scattering at 3087 cm^{-1} exceeds that of the decoupled HOD ν_{OH} vibration.

2.2.4. *Isotopomers decoupled in amorphous ice and the clathrate hydrates*

The first study of the decoupling of the vibrational modes of an icy substance using a few per cent D_2O content was with amorphous ice (Ritzhaupt and Devlin 1977). That early study of the D_2O stretching mode band complex has recently been extended to

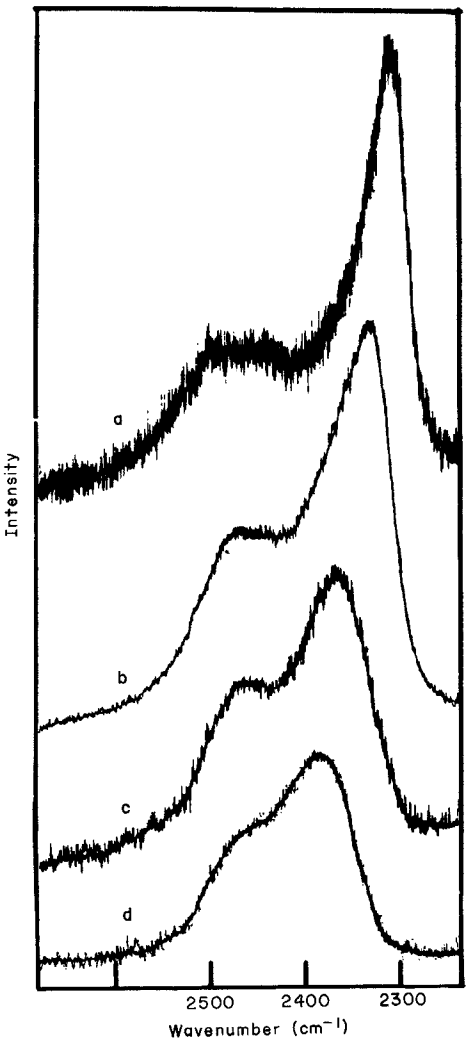

Figure 11. Parallel-polarized Raman scattering for the O–D stretching region of amorphous ice for various concentrations of intact D_2O. Mole percentage D_2O concentrations are: (*a*) 100%; (*b*) 68%; (*c*) 45%; (*d*) 20% (Devlin 1989a).

include the infrared spectra of the decoupled H_2O stretching modes and the bending modes of decoupled HOD and H_2O, with implications regarding the influence of Fermi resonance on the position of ν_1 (Devlin 1989a). Furthermore, isotopic dilution data have been published which reflect the dependence of the polarized Raman spectra of D_2O (or H_2O) on the size of the $(D_2O)_n$ aggregates within amorphous ice (Devlin 1989).

In addition to providing the vibrational frequencies of the decoupled isotopomers in amorphous ice, these decoupling experiments have affirmed the conclusion that intermolecular-coupling effects dominate the amorphous-ice spectrum in the same manner as for crystalline ice I. The parallel-polarized Raman spectra of amorphous ice, for D_2O content ranging from 20 to 80%, are included in figure 11 for comparison with figure 8 of crystalline ice, while the perpendicularly polarized scattering for H_2O

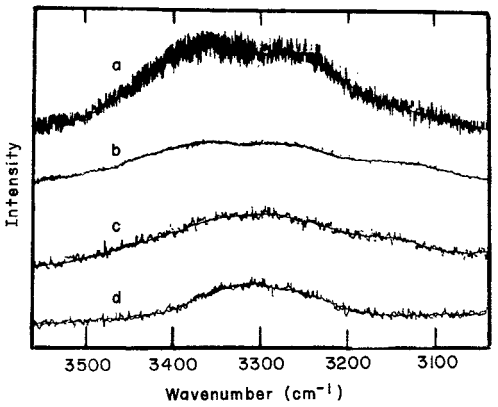

Figure 12. Perpendicularly polarized Raman scattering for the O–H stretching region of amorphous ice for various levels of dilution with intact D_2O. Dilution levels are: (*a*) 0%; (*b*) 20%; (*c*) 45%; (*d*) 88% (Devlin 1989a).

content ranging from 12 to 100%, as presented in figure 12, may be compared with the ice I spectra of figure 10. The sensitivity to dilution of the in-phase-coupled ν_1 mode band position and the convergence of the doublet in the depolarized scattering on the decoupled ν_3 frequency mirror the behaviour observed for ice I. To the extent that this observation is valid, the data indicate that the greater structural disorder of amorphous ice has only a minor effect on the range of the collective behaviour of the coupled vibrational modes.

The isotopically decoupled D_2O modes have also been reported for the structure I hydrates of ethylene oxide (Richardson *et al.* 1985) and trimethylene oxide, and the structure II hydrate of tetrahydrofuran (Fleyfel and Devlin 1988). The results for ethylene oxide and tetrahydrofuran hydrates resemble the corresponding results for ice I except for the greater bandwidths mentioned earlier. For example, it is apparent from curves (*c*) and (*d*) of figure 13 that the decoupled D_2O stretching mode bands of the tetrahydrofuran hydrate have nearly the same splitting and relative intensities as for ice I (figure 6). Since the spectrum of the 100% deuterated hydrate also resembles the corresponding ice spectrum, it follows that the influence of intermolecular coupling on the hydrate spectra is very similar to that for ice I.

The spectra of D_2O isolated in the icy network of the clathrate hydrates are also indicative of relatively subtle structural changes caused by the host–guest interactions. For example, curve (*a*) of figure 13 shows that the isotopically *decoupled* ν_3 mode of the structure I hydrate of trimethylene oxide (TMO) gives rise to a distinct doublet with components at 2478 and 2436 cm^{-1}. This seems to indicate that the D_2O molecules are effectively sorted into two classes as a result of exceptionally large interaction of the TMO molecule with the cage walls, a sorting that does not occur when the cages are occupied by smaller molecules such as ethylene oxide. In fact this hydrate represents the only known icy substance for which a distinct doubling of a *decoupled* stretching mode band has been observed and it is also unique in having a distinct decoupled-stretching-mode band positioned at a frequency lower than for ice I. It can also be noted that the components of the doublet are relatively narrow, substantiating the view that the increased breadth of the clathrate hydrate bands, compared to ice I, is caused

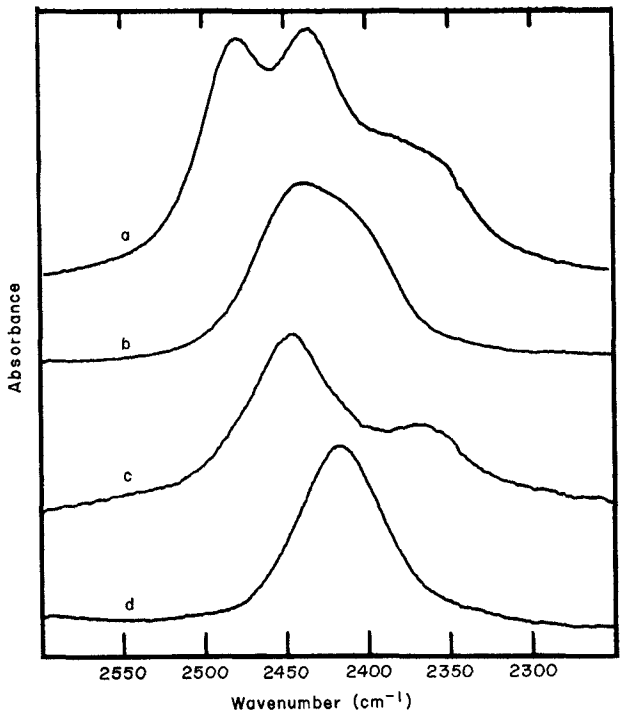

Figure 13. Infrared spectra (90 K) of decoupled D_2O (curves (*a*) and (*c*)) and HOD (curves (*b*) and (*d*)). Curves (*a*) and (*b*) are for the structure I hydrate of TMO while curves (*c*) and (*d*) are for the structure II hydrate of tetrahydrofuran (Fleyfel and Devlin 1988).

by the existence of subsets of hydrogen bonds of different lengths. For the TMO hydrate these subsets apparently group into two larger sets distinguished by their relative O–O distances. For one of these subsets the average O–O distance is greater than for ice I, while the reverse holds for the second set.

2.3. *Large gas-phase clusters of icy substances*

The literature is relatively rich with spectroscopic data for small cold gas-phase and matrix-isolated clusters of water molecules $(H_2O)_n$ where n ranges from two to less than ten, and the techniques used to obtain these data are best suited to the study of small clusters. Only very recently have experimental methods evolved for the routine determination of the complete infrared spectra of large gas-phase molecular clusters (Ewing and De Sheng 1988), including icy clusters (Devlin 1989b, Fleyfel and Devlin 1990). It has been shown that the rapid pressurization of a small precooled gas cell with a gaseous mixture of water vapour diluted with N_2(g), to pressures of a few hundred Torr, results in the efficient formation of icy clusters. At cell temperatures below 100 K, moderate cell pressures and high N_2(g): water dilution ratios, the icy clusters apparently assume an amorphous solid form. For such clusters the infrared band for the O–D stretching mode of decoupled HOD has a position and f.w.h.m. familar from the spectra of thin films of amorphous ice, while the coupled stretching mode spectra

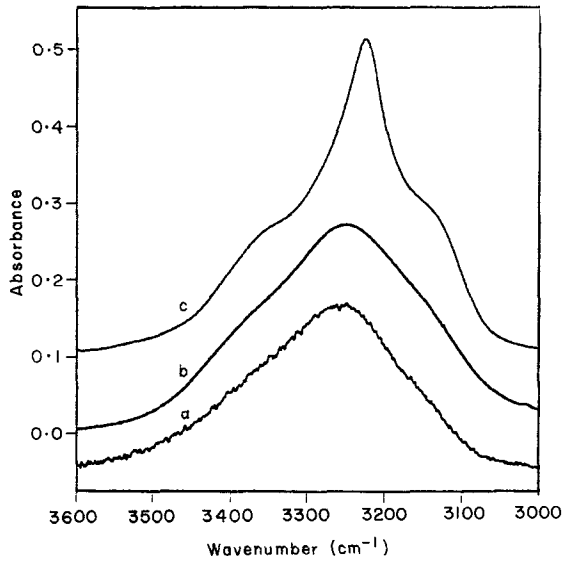

Figure 14. H_2O cluster infrared spectra in the O–H stretching mode region for the indicated temperatures, cell pressures and ratios of the gas components; N_2/H_2O/TMO: (*a*) 100 K, 90 Torr and 600/1/0; (*b*) 170 K, 350 Torr and 100/1/0·08; (*c*) 80 K, 400 Torr and 300/1/0 (Devlin 1989b).

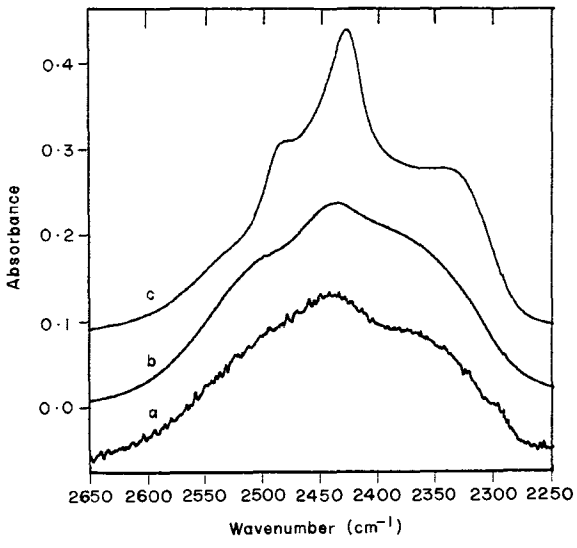

Figure 15. D_2O cluster spectra in the O–D stretching mode region for the indicated temperatures, cell pressures and ratios of the gas components; N_2/D_2O/TMO: (*a*) 80 K, 50 Torr and 200/1/0; (*b*) 170 K, 400 Torr and 100/1/0·12; (*c*) 80 K, 160 Torr and 200/1/0 (Devlin 1989b).

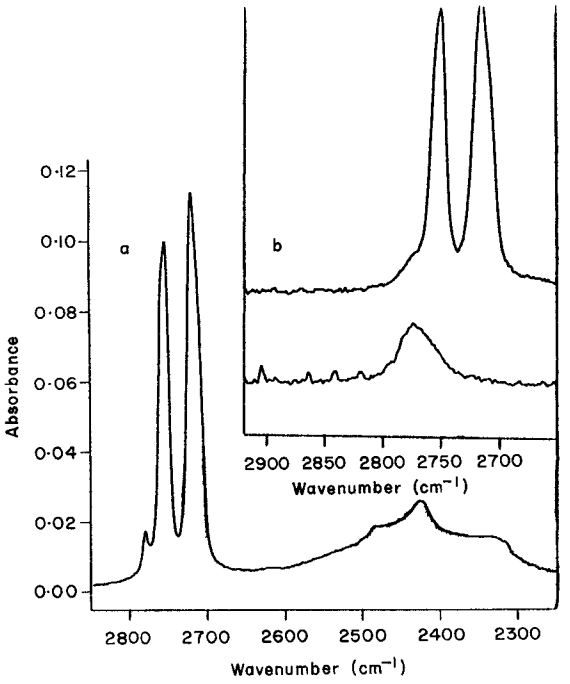

Figure 16. Infrared spectra of clusters of HCl and D_2O at 80 K. Frame (*b*) shows the initial formation of liquid HCl clusters (lower curve) and the crystalline HCl clusters (upper curve) 30 s later. Frame (*a*) shows that loading of the cell with HCl and D_2O through separate ports produces separate and inert HCl and D_2O clusters.

appear as in curves (*a*) of figures 14 and 15. By contrast, the infrared spectra for clusters formed at cell temperatures greater than 100 K, particularly when using higher cell pressures or lower N_2(g) dilution ratios, resembled crystalline ice spectra as is apparent from curves (*c*) in figures 14 and 15. Futhermore, for the latter samples the band of the O–D stretching mode of decoupled HOD had a f.w.h.m. of $\sim 20\,cm^{-1}$ and a peak position of $2415\,cm^{-1}$ at 80 K, both indicative of an ice I structure.

The evidence is that ice I cluster formation is favoured by factors which increase the thermal energy available to the clusters during the formation stage, and that the formation of amorphous solid clusters is somewhat unique to water. In studies of the clustering of small ether and HCl molecules (figure 16), the clusters were observed to form as the supercooled liquids which subsequently crystallized at a rate accelerated by a reduction in cell temperature. This suggests that the water clusters observed in the crystalline form actually nucleated as supercooled liquid clusters, which crystallized instantaneously on the time scale of the spectroscopic observations. If so, the spectra of liquid-water clusters should be observable by sampling at higher temperatures (i.e. ~ 180 K) for which crystal nucleation rates are reduced (Hobbs 1974).

The inclusion of the right concentration of the small ring ether molecules ethylene oxide, trimethylene oxide or tetrahydrofuran in the gaseous water mixtures has been shown to favour the formation of crystalline clathrate hydrate clusters (curves (*b*) of figures 14 and 15). This was definitely so when, for a particular ether, the cell

temperature was chosen to match the value previously shown to be optimum for the preparation of that clathrate hydrate using vapour co-condensation methods.

A comparison of the curves in figures 14 and 15, with the accepted infrared absorption spectra of the stretching mode region of the corresponding icy substances, reveals a distortion in the band complexes of the cluster spectra. This distortion, which is characterized by relatively greater intensity in the higher frequency components of the band complex, has at least three possible sources. Some distortion is undoubtedly present because no correction has been made for anomalous reflectivity effects. It is also possible that the cluster spectra are in fact different from the spectra of the corresponding phase of bulk ice, as is believed to be the case for large CO_2 clusters (Ewing and De Sheng 1988). A third possibility, suggested by data for crystalline HCl clusters, is that the incidence of radiation off-normal to the surfaces of the clusters results in strong absorption by LO modes, in a manner first identified by Berreman (1963) for crystalline thin films. This seems to be the case for the HCl clusters since the intense absorption bands are peaked sharply at the LO frequencies as established by Friedrich and Carlson (1970) for crystalline HCl with very little attenuation of the radiation at the TO band positions (figure 16). Though speculative at this time, this would explain the large excess of intensity at $\sim 2480\,cm^{-1}$ in the crystalline D_2O cluster spectrum (figures 15(*c*) and 27), as that is the position suggested for the ν_3 LO mode by Whalley (and in section 2.2.3 of this review).

2.4. *Implications for water structure*

Though this is not a review about liquid water, a comment about recent advances in understanding the structure of liquid water, based on insights to the spectra of icy substances that have evolved in recent years, seems in order. One of the important conclusions from the theoretical studies by Rice *et al.* (1983) was that some aspects of the intermolecular coupling which so strongly influences the spectra of icy substances are probably retained by liquid water. Green *et al.* (1986a, b, 1987) have subsequently argued that one such aspect is the presence of a collective vibrational mode that, by analogy with ice I and amorphous ice, can be characterized as the delocalized in-phase coupled ν_1 mode.

As mentioned in section 2.1, the most prominent feature of the ice spectra (figures 1 and 5) is the relatively narrow band in the isotropic scattering near $3100\,cm^{-1}$ which experiences a strong shift to higher frequencies with increasing temperature. The assignment of this feature in the Raman spectra of ice I and amorphous ice, to the in-phase-coupled ν_1 collective mode, is apparently accepted without serious challenge. Sceats and co-workers, D'Arrigo *et al.* (1981) and others have helped demonstrate that the Raman spectra of water takes on a similar form with decreasing temperature (figure 17), and it is reasonable to judge that the major differences in the Raman spectra of undercooled water at $-25°C$ and amorphous ice at 130 K would vanish if the two spectra could be obtained at the same temperature. If so, the isotropic scattering on the low-frequency side of the undercooled-water spectrum can also be attributed to a collective mode which develops through the in-phase coupling of the ν_1 fundamental.

From this vantage point Sceats and co-workers have identified the strength of this collective band in the isotropic Raman scattering as a measure of the completeness of the ice-like hydrogen-bonded network. An extrapolation of the collective-mode intensity to lower temperatures indicated that the network is complete (i.e. defect-free) at $\sim -45°C$ since the fraction of the total isotropic scattering intensity included in the

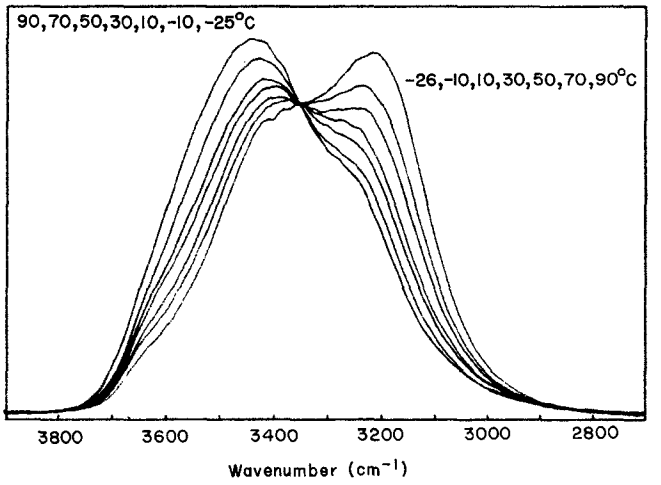

Figure 17. Parallel-polarized Raman scattering of liquid H_2O for temperatures ranging from 90 to −25°C (Green *et al.* 1986).

collective band equals that of ice at that temperature. The collective-mode band intensity is found to be diminished by network defects that can be introduced by the addition of a structure-breaking solute or a temperature increase, and by vibrational decoupling of the oscillators via dilution with an isotopomer. The general approach seems firmly based in the concept of collective modes that has been clearly demonstrated to apply to amorphous ice. However, the model and its extension to the analysis of complex aqueous solutions is not without its detractors.

3. Point defect activities from isotopic exchange rates

The transport of protons along hydrogen-bonded molecular chains is an important phenomenon in nature. Numerous biological processes appear to depend on the transport of protons along or through membranes, possibly along hydrogen bonded chains or 'proton wires' (Nagle *et al.* 1980). Charge separation within ice crystals that ultimately leads to electrical storms undoubtedly depends on proton transport within the hydrogen-bonded network (Gross 1982). Atmospheric chemistry which results in exceptional ozone loss over the polar regions may depend on proton mobility within the acid-rich icy particles of the winter clouds. Fast-ion conductors based on unusual proton mobilities require special proton-transport paths that in some instances resemble proton wires (Schmidt *et al.* 1971). The mobility required for the growth of ice and ice-like crystals, particularly at very low temperatures, may stem from orientational defect activity which is also a pre-requisite for proton transport (Devlin *et al.* 1987). Since the proton transport mechanism has been most thoroughly characterized for ice, scientists in general look to ice as the source of insight to proton transport mechanisms. In this section, attention is directed to spectroscopic studies of isotopic exchange reactions in icy substances that provide the first direct examination of the proton-transport mechanism using a molecular probe.

The spectroscopic data for isotopic exchange of D_2O molecules incorporated into protiated icy substances may, in each instance, be interpreted in terms of the activity of two types of point defects; namely the ionic defects (i.e. OH^- and H^+) and the

orientational, or Bjerrum, defects (i.e. D and L) which have been invoked over the years to interpret ice conductivity data (Hobbs 1974, Camplin *et al.* 1978) and which are inherrent to the theory of Jaccard (1959). The message, that the classical concept of these defects is largely consistent with the exchange data, is part of this review, but no particular effort will be made to consider alternative explanations. Rather, the intent is to (*a*) characterize the isotopic exchange data for pure ice I, amorphous ice and the clathrate hydrates, as well as for icy samples for which the defect activity has been grossly manipulated and (*b*) examine the implications regarding the nature/behaviour of the point defects.

3.1. *FTIR monitoring of the hop and turn steps*

The approach to monitoring defect activity may be conveyed through the spectra of isolated D_2O, HOD and $(HOD)_2$ in figure 6 and the scheme of defect activity shown in figure 18. In the latter figure, the proton and L defects are indicated in the upper drawing, which also includes an isolated D_2O molecule. The L defect is characterized by an O–O linkage with a missing hydrogen atom while the ionic defect is indicated as

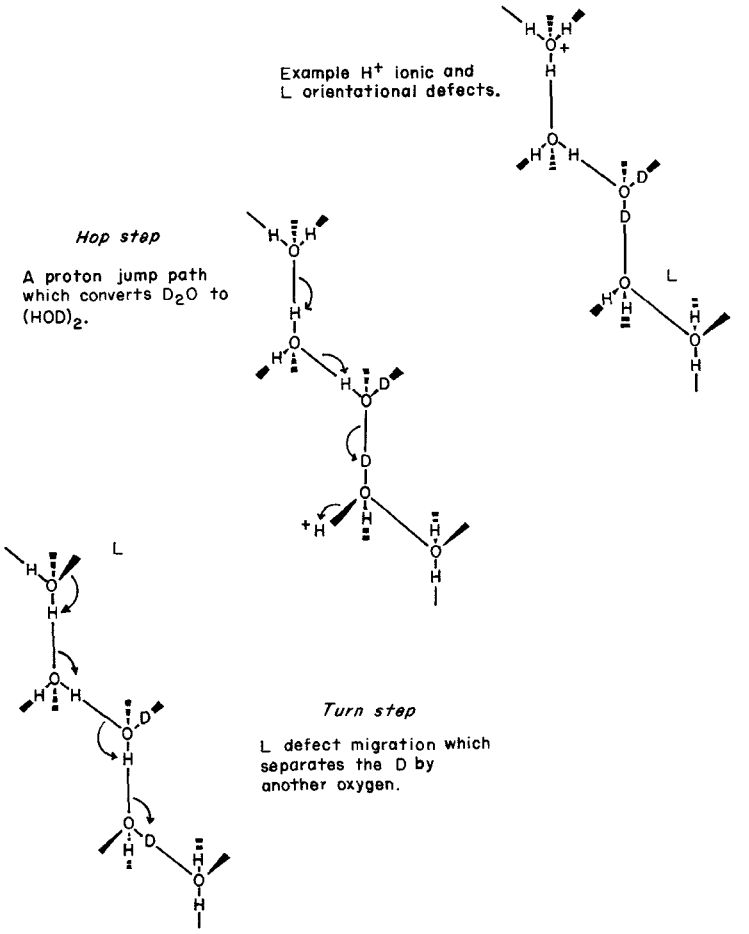

Figure 18. Schematic diagram of the point defects in an ice lattice, showing the proton hop step and the L-defect turn step of proton transport and isotopic exchange.

the oxonium ion, but these entities, even when immobilized, may not be as localized as suggested in the figure (Kashimori *et al.* 1982, Sergienko 1985, Kryachko 1987). In the middle drawing the motion of the proton is characterized as a hop step that converts the isolated D_2O to neighbour coupled HOD (i.e. $(HOD)_2$). It is clear that the rate of this step in a sample is dependent on the concentration and mobility of the protons and, secondly, that proton hopping alone can never remove the two deuterons from neighbouring O–O linkages. This is the molecular-level equivalent of the polarization of a hydrogen-bonded chain by the conduction of a proton (Nagle and Morowitz 1978) so that passage of a second proton is blocked unless the chain is realigned by passage of a Bjerrum defect. The turn step, or L defect passage, is represented in the bottom drawing from which it is clear how separation, and, ultimately, isolation of the deuterons as HOD, can occur at a rate dependent on the concentration and mobility of the L defect.

Several predictions can be made from the point-defect model of figure 18. To simplify the discussion, it is useful to recognize that for pure ice the concentrations of the proton and hydroxide ion are equivalent, as are the L and D defect concentrations, but it has long been believed that the proton and the L defect are the more mobile members of the two pairs. On that basis, it is predictable that base doping of ice will inhibit the hop step, making the first step of figure 18 slow and rate-controlling, so that spectroscopically the isotopic exchange reaction will be observed as the direct conversion of D_2O to isolated HOD. On the other hand, artificial enhancement of the proton concentration should cause the second step in the isotopic exchange reaction to be relatively slow so that reaction is observed as a growth of the $(HOD)_2$ doublet of curve (*b*) of figure 6. Of course, the spectra of samples with a balance of the proton and L defect concentrations and mobilities, for which the rates of the two steps are equivalent, will reveal the successive formation of $(HOD)_2$ and isolated HOD.

The discussion above is applicable to the study of defect activity of any icy substance (as well as ammonia, the ammonia hydrates, etc.) provided a method exists for isolating the deuterated isotopomer within the icy lattice network, and the spectra of the reactant and product isotopomers are unique. This methodology has been demonstrated for ice I_c, amorphous ice and the clathrate hydrates in section 2·2 and has been described for the crystalline dihydrate of ammonia as well (Bertie and Devlin 1983).

3.2. *Pure ice I*

It is difficult, if not impossible, to prepare ice at the purity level required for the study of intrinsic defect activity for temperatures below ~ 200 K. Even at 263 K the proton concentration intrinsic to pure ice has been estimated as $3 \times 10^{16}\,m^{-3}$, and an exponential dependence on the formation energy of several kcal mol^{-1} guarantees vanishing concentrations at very low temperatures (Hobbs 1974). Since the measurements to be examined in this section were made at temperatures below 160 K, it is questionable that the use of thoroughly-degassed triply-distilled water, combined with sample preparation by vapour deposition *in vacuo* at 125 K, provides adequate assurance that the observed defect activity is intrinsic in nature. Nevertheless, some evidence that the results discussed here are indicative of intrinsic defect activity levels will be noted during the review of the results.

The results from spectroscopic monitoring of isotopic exchange in 'pure' ice suggest that ice I, in the temperature range near 145 K, represents the case, referred to above, for which the proton and Bjerrum defect activities are in balance. When pure ice samples,

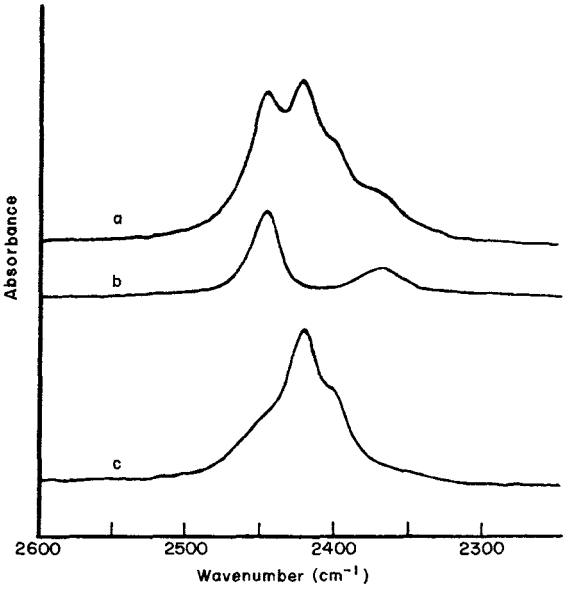

Figure 19. An example for ice I of the resolution of the D_2O–HOD band system into components: (*a*) the composite spectrum after 12 min of reaction at 140 K; (*b*) the pure D_2O curve from figure 6; (*c*) the composite $(HOD)_2$, HOD spectrum obtained by subtracting (*b*) from (*a*) (Collier *et al.* 1984).

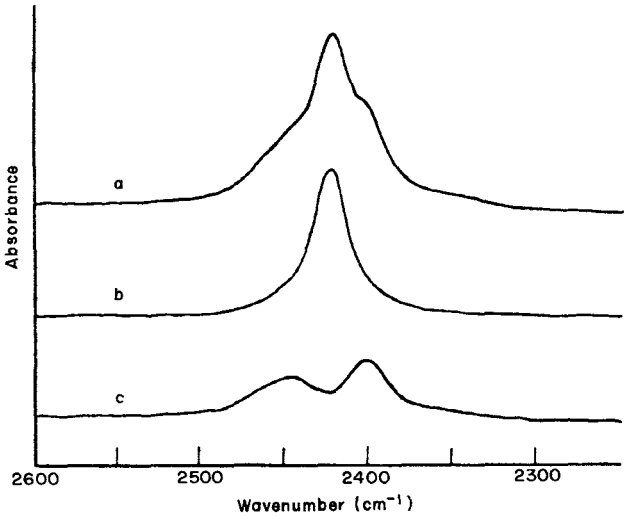

Figure 20. An example of the resolution of the composite $(HOD)_2$, HOD spectrum into components: (*a*) composite spectrum (curve (*c*) of figure 19); (*b*) HOD spectrum from curve (*c*) of figure 6; (*c*) resolved $(HOD)_2$ spectrum (Collier *et al.* 1984).

initially prepared at ~125 K, were warmed into the 145 K range exchange was observed to occur, with the half-life of the isolated D_2O reduced to a matter of several minutes (Collier *et al.* 1984). Furthermore, throughout most of the exchange process $(HOD)_2$, along with isolated HOD, was observable as a product. A typical spectrum of the O–D stretching mode region, obtained after 12 min of exchange at 140 K, is presented as curve (*a*) in figure 19. Subtraction of the D_2O component from curve (*a*) revealed the product curve (*c*) which was readily split into the isolated HOD and $(HOD)_2$ components as in figure 20.

The analysis of curves, such as those in figure 19, as a function of reaction time and at 5 K intervals from 130 to 150 K, established that the hop and turn steps do proceed at comparable rates in this temperature range with the activation energies for hopping and turning evaluated as ~9·5 and ~12·0 kcal mol^{-1} respectively. Though these activation energies are similar to values based on conductivity data obtained at much higher temperatures, the qualitative result that the hop and turn steps occur at a similar rate was not expected. Because of the greater activation energy of the turn step, proton hopping was expected to be faster than the turn step at temperatures below ~200 K. The new result could be attributed to a number of factors, including extrinsic defect activity, the cubic nature of the ice deposits, and/or the fact that the predicted behaviour ignores shallow proton trapping by L defects. The latter phenomenon is a subject of section 3.3.

A testimony to the purity of the ice samples and to the intrinsic nature of the observed defect activity is that, for ice I doped with a trace of organic base (pyridene), the exchange reaction initially proceeded as described above, but with a slowly decreasing rate constant at a given temperature. This observation was believed to reflect the slow, deep trapping of thermally generated protons by exceedingly rare pyridene molecules. Because the decay of the exchange rate occurred on the same time scale as the exchange reaction itself, it hinted that the impurity traps had a concentration comparable to that of the mobile protons, or many orders of magnitude less than the value of 3×10^{16} m^{-3} estimated for $[H^+]$ at 263 K. If pyridene molecules, present at this miniscule concentration level, influence the exchange rate so distinctly, the implication is that impurity levels of the 'pure' samples were vanishingly small and that intrinsic defect activity was observed.

3.3. *Manipulation of the defect activities of ice I*

From the two-step mechanism of complete isotopic scrambling depicted in figure 18, it is clear that the steps may be decoupled and observed independently by manipulation of the relative concentrations of the protons and the L defects. Experience has shown that it is much easier to adjust the concentration of the ionic than the orientational defects. Addition of trace amounts of an organic base, in particular 7-azaindole, to the ice I samples slows the first step by a few orders of magnitude (Ritzhaupt and Devlin 1980) so that the exchange rate proceeds with a half-life of many minutes at 170 K. The base acts as a deep proton trap, so that, with the hop-step rate slow and rate controlling, the concentration of $(HOD)_2$ remains below the detection level for all reaction times (figure 21). This establishes that the hydroxide ion, the concentration of which must increase sharply to maintain the water self-dissociation equilibrium, is an extremely inefficient proton transfer agent (i.e. ineffective as a participant in the hop-step). Nevertheless, in unpublished results it has been found that, although the hop-step is severely depressed by low dopant levels, for heavily base-

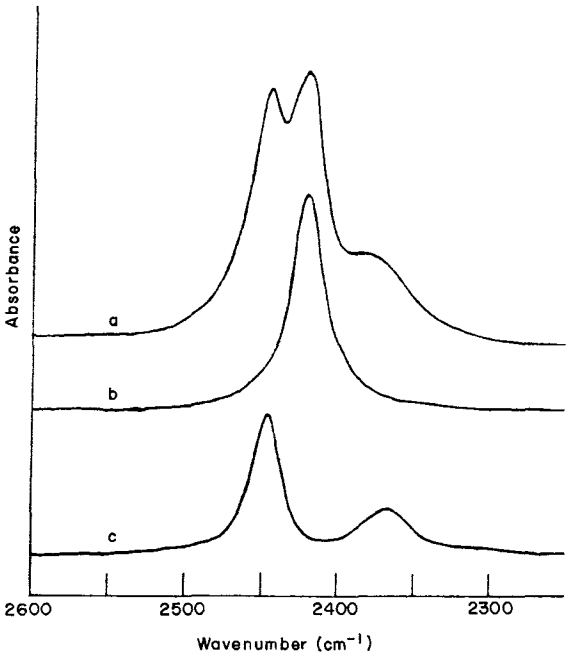

Figure 21. An example of the resolution of the D_2O–HOD band system into the respective components. Data are for a lightly base-doped sample so that the $(HOD)_2$ unit (figure 20(*c*)) does not contribute (Collier *et al.* 1984).

doped ice the hydroxide ion concentration can reach a level at which the hopping rate recovers and exceeds the rate of pure ice (G. Ritzhaupt 1983, unpublished work).

Artificial enhancement of the proton concentration of ice I is possible by several different approaches. The most direct might seem to be the doping with trace amounts of acid, but this is not a practical approach in the present instance because the crystalline samples must be prepared at temperatures (> 120 K) at which the excess protons cause 'instantaneous' isotopic scrambling. Rather, techniques are required for the *in situ* generation of the protons at a reduced temperature, following the formation of the ice I sample. Proton enrichment of samples held below 90 K has been achieved by electron beam bombardment and X-ray irradiation (Devlin and Richardson 1984), the photoconversion of dopant nitrobenzaldehyde to benzoic acid and the ionization of photoexcited dopant molecules such as beta and alpha napthol (Wooldridge and Devlin 1988), and laser-induced single-photon ionization of pure ice (Devlin 1988a).

The influence on defect activities from the different approaches to proton enrichment is qualitatively the same. The excess protons produced below 90 K move only very short distances before becoming localized in shallow traps. They can be subsequently mobilized by warming above 110 K at which temperature the proton hopping step becomes active, and isolated D_2O molecules convert to $(HOD)_2$. At this temperature, even for the samples damaged by electron-beam bombardment, there are no mobile L defects in the ice I samples so conversion of $(HOD)_2$ to isolated HOD is prohibited and the $(HOD)_2$ becomes the dominant deuterated molecular species (see the top curve of figure 22).

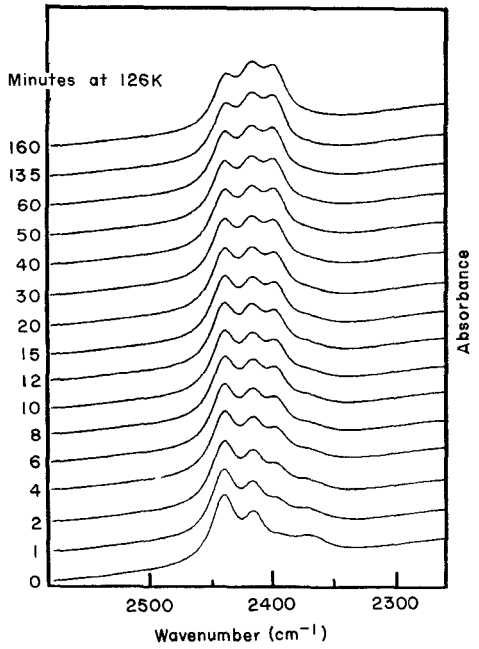

Fig. 22. Time dependence of the infrared spectrum of ice I in the O–D stretching region following 2 h of u.v. irradiation at 90 K. The spectra, from bottom to top, reflect the conversion of isolated D_2O to $(HOD)_2$ at 126 K (Wooldridge and Devlin 1988).

This observation of the shallow trapping of protons seems to confirm an earlier report of Kunst and Warman (1983) that pulsed irradiolysis of ice at ~260 K results in mobile protons in pseudo-equilibrium with protons immobilized in shallow traps. They identified the localization of the protons as a complexation with the L defects; a reasonable choice since an L defect has an associated negative charge of $\sim 0{\cdot}37e$ (Hubmann 1979, Scheiner and Nable 1983). However, for those experiments for which the proton enrichment is achieved using radiation that damages the ice lattice and produces new chemical species, it is not obvious that the trapping is an intrinsic property of ice. For this reason, the observation, that protons produced by single-photon vibrational excitation are also shallow trapped (Devlin 1988b), is significant support of the view that shallow trapping is an inherent property of ice that may involve the complexation of the protons with the L defects.

The binding energy of the proton L defect complex was originally estimated by Kunst and Warman from microwave conductivity measurements and, more recently, by Wooldridge and Devlin from the rates of isotopic exchange reactions caused by the mobile protons in pseudo-equilibrium with complexed (trapped) protons. For ice I, but apparently not other icy substances (Richardson *et al.* 1985b), the temperature dependence of the proton hop-step rate can be related directly to the enthalpy change for the complexation. Using spectroscopic data (figure 22) reflecting the rate of conversion of isolated D_2O to $(HOD)_2$, a binding energy of $10{\cdot}0\,\text{kcal mol}^{-1}$ was estimated, in reasonable agreement with the earlier values of $12{\cdot}6\,\text{kcal mol}^{-1}$.

The firm evidence that shallow proton traps exist in ice suggests that there is an 'activation energy' for proton transfer even for pure ice, with the fraction of protons that are active at a given temperature determined by the trap depth. Knowledge of the magnitude of this energy is apparently basic to any understanding of the temperature dependence of proton-transfer processes, including the conductivity of icy substances. This suggests a need for a significant modification of the usual application of Jaccard's theory to the analysis of conductivity data. Recently, modern conductivity results for ice doped with HCl (Takei and Maeno 1984, 1987, Gross *et al.* 1978), which had originally been analyzed without accounting for proton L defect complexation, have been re-interpreted to emphasize the implications of proton shallow trapping (Devlin 1988a).

The exchange reaction at ~ 120 K, caused by the protons released from the shallow traps, occurs without L defect activity and thus reflects a decoupling of the hop and turn steps. It also leaves the ice sample in a form that is ideal for monitoring the turn step since most of the deuterium is present as $(HOD)_2$, as is clear from figure 22. The subsequent warming of such samples into the 130–150 K range allows a rather direct observation of the normal turn-step activity, independently of the hop step. An example of the influence of the thermally activated turn step on the $(HOD)_2$ concentration at 145 K is given in figure 23 with the conversion to isolated HOD occurring with a half-life of less than 0·5 h. Data such as these are useful for re-evaluation of the activation energy of the turn step and have provided assurance that the correct value is close to 12·0 kcal.

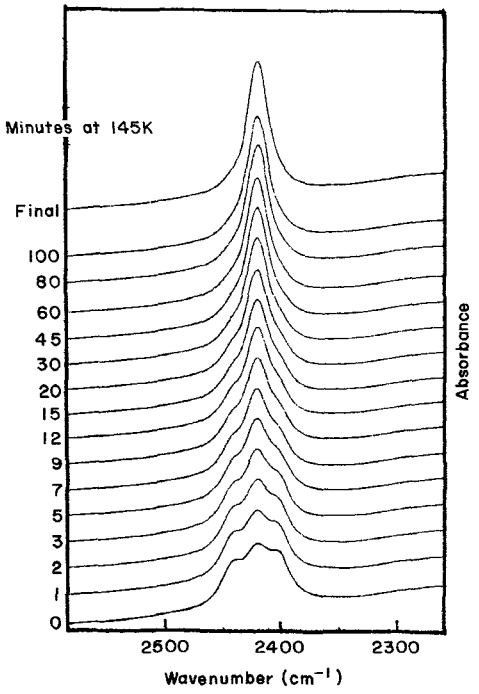

Figure 23. Time dependence of the infrared spectrum of ice I at 145 K following the 126 K conversion of isolated D_2O to a 4:1 equilibrium mixture of $(HOD)_2$ and D_2O (figure 22). The spectra, bottom to top, reflect the conversion to isolated HOD (Wooldridge and Devlin 1988).

This ability to fully decouple the hop and turn steps of the exchange (and conduction) process provides a level of confirmation of the theory of Jaccard. No doubt remains that two different entities within ice I participate in the transport of charge, and the nature of the entities is consistent with their identification as the proton and the L defect having properties envisioned by the theory. On the other hand, the intrinsic shallow trapping of protons, perhaps by the L defects, suggest that the ionic and orientational defects do not behave independently, and that recognition of the existence of the proton shallow traps, which clearly dictates the proton behaviour at low temperatures, is necessary in the routine analysis of the charge-transport data of icy substances.

3.4. *Amorphous ice and clathrate hydrates*

There has been only one in-depth study of the isotopic exchange reaction in a clathrate hydrate (Richardson *et al.* 1985b). Because the crystalline structure I hydrate of ethylene oxide can be prepared at 100 K by the co-deposition of water and the ether vapours at a $\sim 6:1$ ratio, it is possible to grow the hydrate with intact isolated D_2O incorporated. Since a second species, ethylene oxide, must be deliberately included in the deposit, the achievement of adequate sample purity for observation of intrinsic defect activity becomes even more unlikely than for ice I. Nevertheless, a consistent pattern of defect activity emerged for the ethylene-oxide hydrate. The hydrate is much more proton-active than ice with the hopping step rate at 115 K comparable to the rate for ice at 145 K. Despite this greater hop rate, the hop step of figure 18 was observed to be slow compared to the turn-step rate, as evidenced by a direct conversion of D_2O to fully isolated HOD.

As for ice I, knowledge of the spectra of isolated D_2O, $(HOD)_2$, and isolated HOD (figure 24) were a pre-requisite for an interpretation of the exchange-rate data. The spectra of figure 25, obtained by subtracting an appropriate amount of HOD-band

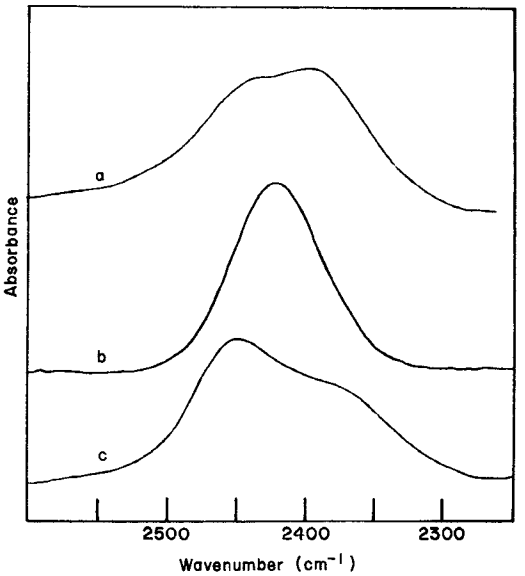

Figure 24. Infrared absorbance curves (10 K) for (*a*) $(HOD)_2$, (*b*) HOD and (*c*) D_2O in the O–D stretching region of the ethylene oxide clathrate hydrate (Richardson *et al.* 1985c).

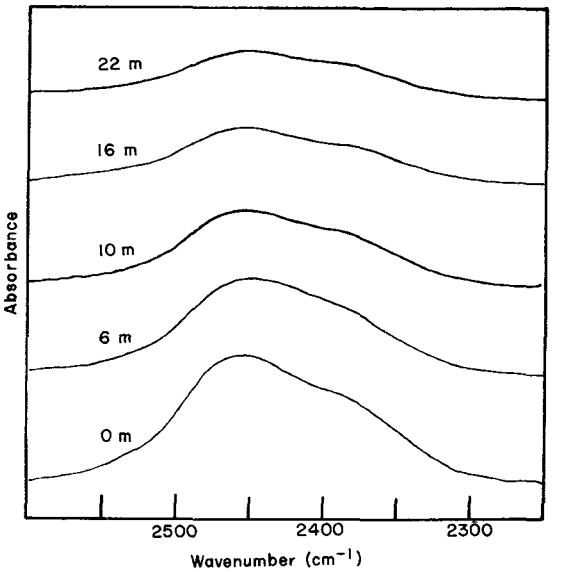

Figure 25. Time variation of the intensity of the D_2O stretching mode absorption bands of the ethylene oxide clathrate hydrate for isotopic exchange at 118 K (Richardson *et al.* 1985c).

intensity in each case, reflect the direct conversion of D_2O to isolated HOD, since there is no evidence of the $(HOD)_2$ intermediate. The high rate of the turn step for this hydrate is predictable from the known orientational relaxation rate of the host ice lattice which exceeds that of ice I by orders of magnitude (Davidson and Ripmeester 1984). If orientational relaxation is dependent on mobile orientational defects, as concluded by Johari and Jones (1976), the much greater relaxation rate is evidence of a relatively high population of mobile L defects. The isotopic exchange data seem to confirm this view.

It was possible to obtain qualitative information on the turn-step rate by observing the exchange process in a crystalline hydrate sample after electron beam bombardment. At temperatures below $\sim$70 K the protons produced by the electron beam converted isolated D_2O to $(HOD)_2$. Upon warming to $\sim$90 K the turn step was activated and the $(HOD)_2$ converted to isolated HOD. As for ice I, this represents a clean separation of the exchange reaction into two steps, one dependent on mobile protons and the second a result of orientational defect activity. The spectrum of $(HOD)_2$ in figure 24 was made possible by this selective activation of the point defects.

It is particularly interesting that the activity of the L defects within the clathrate hydrate of ethylene oxide at 90 K compares favourably with the activity in ice I at 140 K. It has been suggested that this much greater defect activity may be the source of the molecular mobility in the ethylene-oxide clathrate hydrate that permits growth by vapour co-condensation at the remarkably low-temperature of 100 K (Wooldridge *et al.* 1987). No other icy crystalline substance has been observed to grow by vapour deposition, even epitaxially, at this temperature. A lengthy argument, based on circumstantial evidence, that the low-temperature growth of crystalline icy substances depends, in general, on the presence of mobile orientational defects, has been

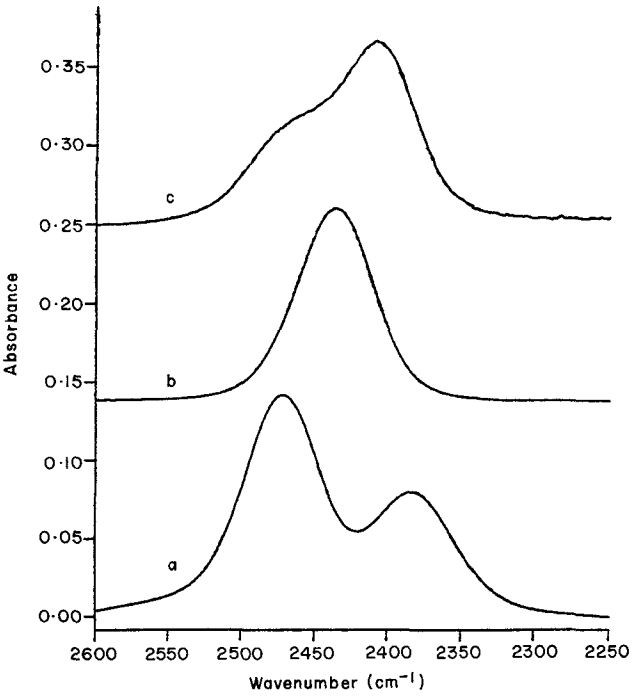

Figure 26. Infrared absorbance curves (80 K) for (*a*) D_2O, (*b*) HOD and (*c*) $(HOD)_2$ in the O–D stretching region of amorphous ice (Fisher and Devlin 1989).

developed. A critical part of that argument is the firm evidence that the temperature of the onset of the L defect mobility in ice I (section 3.2) matches the crystallization temperature of amorphous ice of ~ 145 K (on a time scale of several minutes).

There has been some hesitance to describe defects in amorphous ice in the same terms as for crystalline ice I, but the spectroscopic monitoring of the isotopic exchange reaction has now provided solid evidence that the transfer of charge in amorphous ice is properly described in terms of separate charge carriers, namely mobile protons and L defects (M. Fisher and J. P. Devlin 1989, unpublished work). The exchange data for pure amorphous ice are not particularly interesting, since mobile protons are lacking at temperatures at or below the crystallization temperature. With the first exchange step inactive, the second step is not observable, so in essence D_2O remains intact in pure amorphous ice until crystallization occurs. However, as for the other icy substances, the proton concentration of amorphous ice can be enhanced artificially.

No quantitative rate data are yet available, but unpublished results show that amorphous ice containing a trace of beta-napthol becomes proton active when protolyzed with a mercury resonance lamp at ~ 80 K. Consequently, isolated D_2O is converted to $(HOD)_2$, the spectrum of which is presented in figure 26(*c*). Warming of the sample to ~ 100 K activates the L defects so that isolated HOD (figure 26(*b*)) becomes the ultimate product. As for the ethylene-oxide clathrate hydrate, the exchange data clearly reveal that amorphous ice is rich with mobile L defects compared to crystalline ice I. Since the protons are subject to shallow trapping by these abundant

L defects, it is understandable that vapour deposits of amorphous ice containing high concentrations of ionized nitric acid contain no mobile protons at temperatures below ~90 K (D. Wilkinson and J. P. Devlin 1989, unpublished work).

The thermal activation of mobile L defects at temperatures above 100 K is noteworthy, since high-density amorphous ice converts to low-density amorphous ice at ~114 K (Handa and Klug 1988). A possible implication is that the low-density amorphous ice cannot form without the influence of orientational defects which are active on a laboratory time scale. This is also near the minimum temperature at which it is possible to anneal away the excess enthalpy of vapour-deposited amorphous ice, which may suggest that the structural relaxation involved is similarly dependent on defect activity. Further, these insights to the L defect and its activity prompt the suggestion that the glass-transition temperature of ~124 K, which has been established by Handa and Klug for amorphous ice, reflects the activation of an orientational mode dependent on the presence of mobile L defects. Such a viewpoint seems to be consistent with the thinking of Yamamuro *et al.* (1987a, b, 1988) with respect to the glass-transition temperatures they have identified for various phases of ice. Certainly, their T_g value for cubic ice (140 K) closely matches both the temperature of onset of L defect activity as discussed above, and the crystallization temperature of ice I_c from amorphous ice.

3.5. *Ice I clusters*

Research on point-defect activities in large gas-phase icy clusters is in its infancy. The quantitative application of the techniques described in section 3.1 awaits the development of a cluster cell designed for the incorporation of isolated D_2O in icy H_2O clusters. However, preliminary results have been reported for the reaction of H_2O ice I clusters with D_2O ice I clusters (Devlin 1989c). When the cluster cell is pressurized by

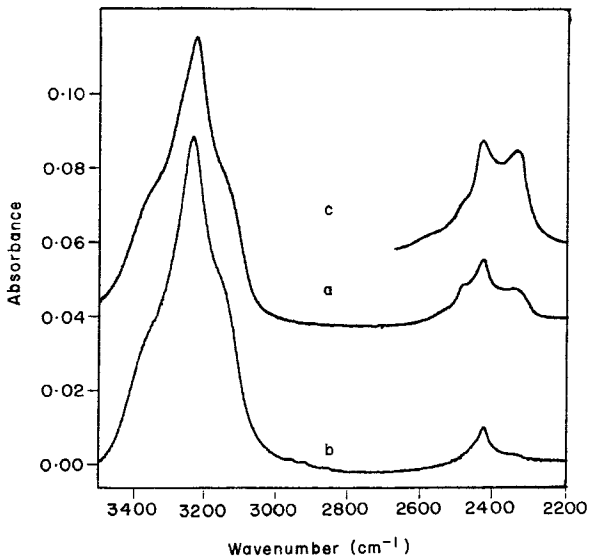

Figure 27. H_2O and D_2O cluster spectra for simultaneous separate loading of H_2O and D_2O gaseous mixtures with N_2: (*a*) 200/1 mixtures loaded at 90 K to a pressure of 200 Torr; (*b*) 200/1 mixtures loaded at 140 K to a pressure of 260 Torr and held for 10 min; (*c*) crystalline ice I spectrum (150 K) redrawn from figure 21 of Sceats and Rice (1982).

the simultaneous admission of two gaseous mixtures (N_2/H_2O and N_2/D_2O) through separate portals spaced by 4 cm, the clusters also form separately and produce a spectrum (figure 27 (*a*)) which is the composite of the single isotopomer cluster spectra of figures 14 (*c*) and 15 (*c*). If the cluster formation occurs in a cell cooled to 120 K or lower, the clusters are inert and the spectra are invariant with time. Neither isotopic dilution nor exchange occurs during or after cluster formation. However, when the separate clusters are formed at 140 K, isotopic exchange occurs rapidly as reflected by a growth of the O–D band of isolated HOD, as in figure 27 (*b*).

This isotopic exchange, between the separately formed H_2O and D_2O crystalline clusters, requires the transfer of water molecules between colliding ice clusters, as well as activity by both types of point-defects, to produce isolated HOD. Such results give qualitative information about defect activity, including an indication that the activity in clusters is apparently greater than for bulk ice. The transfer of molecules through cluster collisions is itself of some interest, and it is easy to envision experiments, based on the separate formation of different types of clusters, for study of the rate of proton transfer between clusters. The spectrum of figure 16 (*a*), which reflects the separate formation of inert D_2O ice I clusters and crystalline clusters of HCl at 80 K, can be viewed as a step in that direction. Were the D_2O molecules isolated in H_2O ice I clusters, and the HCl ionized in separate H_2O ice clusters, the rate of D_2O conversion to $(HOD)_2$ could be followed as a gauge of the proton transfer rate between clusters.

4. Summary

The spectroscopic study of point defects has clearly revealed the separate existence and effects of two types of defects within icy substances, including amorphous ice. There is no reason, from these data, not to identify the defect responsible for proton hopping with the proton itself, while the second defect functions as expected for the orientational L defect. In this respect, as well as from evidence that the hydroxide ion facilitates proton hopping for *high* base concentrations in ice I and amorphous ice, the results for isotopic exchange satisfy the expectations of the Jaccard theory. However, confirmation that protons in ice are of two types, mobile and shallowly trapped, so that the proton mobility is activated in a complex manner which appears to depend on the binding energy of the proton with the L defect (and, by implication, the temperature dependence of the L defect population), may require modification of the theory to interpret properly proton-transport data.

The exchange data also clearly establish that the L defect activity varies by orders of magnitude for different icy substances. This difference can be conveyed by the observation that the half-life for passage of an L defect through an average lattice site (i.e. an $(HOD)_2$ unit) is similar for ice, amorphous ice and the ethylene-oxide clathrate hydrate for the temperatures 145 K, 110 K and 90 K respectively. It has been proposed that this L defect activity determines the ability of a substance to form at a given temperature, a possibility which is a continuing area of investigation. However, Mayer (1988, private communication) found no effect on the devitrification temperature of glassy water from the presence of either ammonia (10^{-2} M) or HCl (10^{-3} M).

Because the Bjerrum-defect concentrations exceed the ionic-defect concentrations by many orders of magnitude (Hobbs 1974), the proton activity of ice I is more easily adjusted than is the L defect activity. Nevertheless, the addition of HCl to ice might appear to automatically increase the L defect concentration and activity. However, much of the HCl may be excluded during crystal formation and, of that part which is incorporated, a proton is introduced along with each L defect (assuming complete

ionization of the HCl). The L defects apparently complex with the protons and are probably immobilized (Hubmann 1979) so that the net increase in L defect activity may be minimal. On the other hand, based on the orientational relaxation times, with confirmation from isotopic exchange data, the L defect activity of the clathrate hydrates may be adjusted by orders of magnitude by the choice of the guest molecule. For this reason, these hydrates represent a fertile area for investigation of the influence of the L defect activity on properties such as relative crystal growth rates.

References

BERGREN, M. S., and RICE, S. A., 1982, *J. chem. Phys.*, **77**, 583.

BERREMAN, D. W., 1963, *Phys. Rev.*, **6**, 2193.

BERTIE, J. E., and DEVLIN, J. P., 1983, *J. chem. Phys.*, **78**, 6203; 1984, *Ibid.*, **88**, 380.

BERTIE, J. E., and OTHEN, D. A., 1972, *Can. J. Chem.*, **50**, 3443; 1973, *Ibid.*, **51**, 1159.

CARMONA, P., AOUIZERAT-ELARBY, A., JAL, J. F., DUPUY, J., CROSET, B., and CHIEUX, P., 1989, *Phase Transitions*, **14**, 11.

CAMPLIN, G. C., GLEN, J. W., and PAREN, J. G., 1978, *J. Glaciol.*, **21**, 123.

COLLIER, W. B., RITZHAUPT, G., and DEVLIN, J. P., 1984, *J. phys. Chem.*, **88**, 363.

DAVIDSON, D. W., 1973, *Water, a Comprehensive Treatise*, volume 2, edtied by F. Franks (New York: Plenum), chap. 3.

DAVIDSON, D. W., and RIPMEESTER, J. A., 1984, *Inclusion Compounds III*, edited by J. L. Atwood, J. E. D. Davis and D. D. MacNicol (New York: Academic), chap. 3.

D'ARRIGO, G., MAISANO, G., MALLAMACE, F., MIGLIARDO, P., and WANDERLINGH, F., 1981, *J. chem. Phys.*, **75**, 4264.

DEVLIN, J. P., and FRECH, R., 1975, *J. chem. Phys.*, **63**, 1663.

DEVLIN, J. P., and RICHARDSON, H. H., 1984, *J. chem. Phys.*, **81**, 3250.

DEVLIN, J. P., 1988a, *J. chem. Phys.*, **89**, 5967; 1988b, *J. phys. Chem.*, **92**, 6867; 1989a, *J. Chem. Phys.*, **90**, 1322; 1989b, *J. molec. Struct.* (in the press); 1989c, *J. chem. Phys.*, **91**, 5850.

DEVLIN, J. P., WOOLDRIDGE, P. J., and RITZHAUPT, G., 1986, *J. chem. Phys.*, **84**, 6095.

EFIMOV, Y. Y., 1982, *J. struct. Chem.*, **23**, 407.

EWING, G. E., and DE SHENG, T., 1988, *J. phys. Chem.*, **92**, 4062.

FALK, M., 1984, *Spectrochim. Acta* A, **40**, 43; 1987, *J. chem. Phys.*, **87**, 28.

FLEYFEL, F., and DEVLIN, J. P., 1988, *J. phys. Chem.*, **92**, 631; 1990, *J. chem. Phys.*, **92**, 34.

FRIEDRICH, H. B., and CARLSON, R. E., 1970, *J. chem. Phys.*, **53**, 4441.

GREEN, J. L., LACEY, A. R., and SCEATS, M. G., 1986a, *J. phys. Chem.*, **90**, 3961; 1986b, *Chem. phys. Lett.*, **130**, 67; 1987, *J. Phys., Paris*, **48**, C1–53.

GROSS, G. W., HAYSLIP, I. C., and HOY, R. N., 1978, *J. Glaciol.*, **21**, 143.

GROSS, G. W., 1982, *J. geophys. Res.*, **87**, C9, 7170.

HAAS, C., and HORNIG, D. F., 1960, *J. chem. Phys.*, **32**, 1763.

HANDA, Y. P., and KLUG, D. D., 1988, *J. phys. Chem.*, **92**, 3323.

HUBMANN, M., 1979, *Z. Phys.* B, **32**, 127.

HWANG, D. M., 1974, *Phys. Rev.*, **9**, 2717.

JACCARD, C., 1959, *Helv. phys. Acta.*, **32**, 89.

JOHARI, G. P., and CHEW, H. A. M., 1983, *Nature*, **303**, 604.

JOHARI, G. P., and JONES, S. J., 1976, *Proc. R. Soc. Lond.* A, **349**, 467.

LI, P. C., and DEVLIN, J. P., 1973, *J. chem. Phys.*, **59**, 547.

KASHIMORI, Y., KIKUCHI, T., and NISHIMOTO, K., 1982, *J. chem. Phys.*, **77**, 1904.

KRYACHO, E. S., 1987, *Chem. phys. Lett.*, **141**, 346.

KUNST, M., and WARMAN, J. M., 1983, *J. phys. Chem.*, **87**, 4093.

MCGRAW, R., MADDEN, W. G., BERGREN, M. S., RICE, S. A., and SCEATS, M. G., 1978, *J. chem. Phys.*, **69**, 3483.

NAGLE, J. F., MILLE, M., and MOROWITZ, H. J., 1980, *J. chem. Phys.*, **72**, 3959.

NAGLE, J. F., and MOROWITZ, H. J., 1978, *Proc. Natl Acad. Sci. U.S.A.*, **75**, 298.

PLUMMER, P. L. M., 1978, *J. Glaciol.*, **21**, 565.

RICE, S. A., BERGREN, M. S., BELCH, A. C., and NIELSON, G., 1983, *J. phys. Chem.*, **87**, 4295.

RICHARDSON, H. H., WOOLDRIDGE, P. J., and DEVLIN, J. P., 1985a, *J. chem. Phys.*, **83,** 4387; 1985b, *J. phys. Chem.*, **89,** 3552.
RITZHAUPT, G., and DEVLIN, J. P., 1977, *J. chem. Phys.*, **67,** 4779; 1980, *Ibid.*, **72,** 6807.
RITZHAUPT, G., THORNTON, C., and DEVLIN, J. P., 1978, *Chem. phys. Lett.*, **59,** 420.
RITZHAUPT, G., COLLIER, W. B., THORNTON, C., and DEVLIN, J. P., 1980, *Chem. phys. Lett.*, **70,** 294.
SCEATS, M. G., STAVOLA, M., and RICE, S. A., 1979, *J. chem. Phys.*, **71,** 983.
SCEATS, M. G., and RICE, S. A., 1982, *Water, a Comprehensive Treatise*, volume 7, edited by F. Franks (New York: Plenum), chap. 2.
SCHEINER, S., and NAGLE, J. F., 1983, *J. phys. Chem.*, **87,** 4267.
SCHERER, J. R., 1978, *Advances in Infrared and Raman Spectroscopy*, volume 5, edited by R. J. H. Clark and R. E. Hester (Chichester: John Wiley and Sons) chap. 3.
SCHERER, J. R., and SNYDER, R. G., 1977, *J. chem. Phys.*, **67,** 4794.
SCHMIDT, V. H., DRUMHELLER, J. E., and HOWELL, F. L., 1971, *Phys. Rev.* B, **4,** 4582.
SERGIENKO, A. I., 1985, preprint from the Academy of Sciences of the Ukrainian S.S.R., Institute for Theoretical Physics.
SIVAKUMAR, T. C., CHEW, H. A. M., and JOHARI, G. P., 1978, *Nature*, **275,** 524.
SIVAKUMAR, T. C., RICE, S. A., and SCEATS, M. G., 1978a, *J. chem. Phys.*, **69,** 3468.
SIVAKUMAR, T. C., SCHUH, D., SCEATS, M. G., and RICE, S. A., 1977, *Chem. phys. Lett.*, **48,** 212.
TAKEI, I., and MAENO, N., 1984, *J. chem. Phys.*, **81,** 6186; 1987, *J. Phys., Paris*, **48,** C1–121.
WHALLEY, E., 1977, *Can. J. Chem.*, **55,** 3429.
WHALLEY, E., and KLUG, D. D., 1979, *J. chem. Phys.*, **71,** 1513; 1986, *Ibid.*, **84,** 78; 1987, *Ibid.*, **86,** 7244.
WONG, P. T. T., and WHALLEY, E., 1975, *J. chem. Phys.*, **62,** 2418.
WOOLDRIDGE, P. J., and DEVLIN, J. P., 1988, *J. chem. Phys.*, **88,** 3086.
WOOLDRIDGE, P. J., RICHARDSON, H. H., and DEVLIN, J. P., 1987, *J. chem. Phys.*, **87,** 4126.
YAMAMURO, O., OGUNI, M., MATSUO, T., and SUGA, H., 1987a, *Solid-St. Commun.*, **62,** 289; 1987b, *J. phys. Chem. Solids*, **48,** 935; 1988, *Ibid.*, **49,** 425.
ZHIZHIN, G. N., and GONCHAROV, A. F., 1984, *Vibrational Spectra and Structure*, volume 13, edited by J. R. Durig (Amsterdam: Elsevier), chap. 5.